Energetically consistent Eddy-Diffusivity Mass-Flux convective schemes. Part I: Theory and Models.

Manolis Perrot, Florian Lemarié, Thomas Dubos

Energetically consistent Eddy-Diffusivity Mass-Flux convective schemes. Part I: Theory and Models.

M. Perrot[1,*], F. Lemarié[1], T. Dubos[2]

[1]Univ. Grenoble Alpes, Inria, CNRS, Grenoble INP, LJK, Grenoble, France
[2]IPSL, Lab. Meteorologie Dynamique, Ecole Polytechnique, Palaiseau, France

Key Points:

- An Eddy-Diffusivity Mass-Flux parameterization is carefully derived from first principles, making the underlying assumptions explicit
- Closed bulk energy budgets between resolved and subgrid energy reservoirs are outlined using modern anelastic and Boussinesq energetics
- Energy budgets and mass-flux hypotheses motivates the consistent formulation of TKE equation, boundary conditions and transport of TKE

Corresponding author: Manolis Perrot, `manolis.perrot@univ-grenoble-alpes.fr`

Abstract

This paper provides a self-contained derivation from first principles of a convective vertical mixing scheme rooted in the Eddy-Diffusivity Mass-Flux (EDMF) approach. This type of closure involves separating vertical turbulent fluxes into two components: an eddy-diffusivity (ED) term that addresses local small-scale mixing in a near isotropic environment, and a mass-flux (MF) transport term that accounts for the non-local transport performed by vertically coherent plumes within the environment. Using the multi-fluid averaging underlying the MF concept, we review consistent energy budgets between resolved and subgrid scales for seawater and dry atmosphere, in anelastic and Boussinesq settings. We show that when using an EDMF scheme, closed energy budgets can be recovered if: (*i*) bulk production terms of turbulent kinetic energy (TKE) by shear, buoyancy and transport include MF contributions; (*ii*) boundary conditions are consistent with EDMF, to avoid spurious energy fluxes at the boundary. Moreover we show that lateral mixing due to either entrainment or detrainment induces a net production of TKE via the shear term, and such production is enhanced when horizontal drag increases. Throughout the theoretical development of the scheme, we maintain transparency regarding underlying assumptions. In a companion paper (Perrot and Lemarié (2024); hereafter Part II) we assess the validity of such hypotheses and the sensitivity of the scheme to modelling choices against Large Eddy Simulations (LES) and observational data of oceanic convection, detail an energy-conserving discretization, and quantify energy biases of inconsistent formulations.

Plain Language Summary

In Earth system models, various important processes occur on scales that are too fine to be resolved with usual grid resolutions. Parameterizations have to be used to approximate the average effect of such processes on the scales resolved by a numerical model. The general objective of the proposed work is to approach the parameterization problem for boundary-layer turbulence and convective plumes in a "consistent" manner. Here the notion of consistency integrates various aspects: global energetic consistency, consistency with a particular averaging technique for the scale-separation, and the rigorous reduction of a physical system to a scale-aware parametric representation based on well-identified and justifiable approximations and hypotheses. An originality is to jointly consider energy budgets including a subgrid energy reservoir on top of the resolved energies allowing the proper coupling between the parameterization and the resolved fluid dynamics. This research is fundamental to reduce energy biases in models, and to pave the way toward an alternative methodology to parameterize oceanic convection across scales. In a companion paper, numerical simulations demonstrate the adequacy of the proposed parameterization.

1 Introduction

1.1 Convection in the ocean and atmosphere and its parameterization in numerical models

Boundary layer convection occurs in the atmosphere and the ocean due to buoyancy fluxes at the surface, which trigger gravitational instabilities. Buoyant plumes then tend to overturn and mix the fluid. When looking at the mean properties of the fluid, it leads to the formation of a well-mixed layer. The accurate representation of such boundary layers is of paramount importance for short-term forecasts as well as for climate projections in the atmosphere (Bony et al., 2015; Schneider et al., 2017) and the ocean (Martin et al., 2013; Piron et al., 2016; Moore et al., 2015; Fox-Kemper et al., 2019). Regarding current computational capacities, plumes are still unresolved in regional and global numerical models, and thus their effects require parameterization. Moreover in ocean modeling, beyond the requirement in terms of grid resolution, hydrostatic equations used in

the overwhelming majority of regional and global studies are not suitable for resolving convective phenomena explicitly (Marshall et al., 1997).

For any quantity X, standard turbulent mixing models are based on the closure of vertical turbulent fluxes $\overline{w'X'}$ proportional to the local (in height) mean gradient in the form $-K_X \partial_z \overline{X}$ which corresponds to the so-called Eddy-Diffusivity (ED) closure (where w is vertical velocity, z is the vertical height and $\overline{(.)}$ is a Reynolds average). Such a closure leads to a diffusion of $\overline{X}$, which is often justified by considering that turbulent fluctuations resemble Brownian motion (Vallis, 2017; Resseguier et al., 2017). Although the ED closure has been widely used in many industrial and geophysical applications, it is known to potentially predict incorrectly higher order moments and even mean fields for complex flows (e.g. Schmitt, 2007). For instance, the inadequacy of ED closures for atmospheric convection has long been highlighted (Deardorff, 1966). Indeed fluctuations are carried by non-local structures, the buoyant plumes, that can be coherent over the whole mixed layer. In particular, in such a layer, mean gradients are close to zero ($\partial_z \overline{X} \simeq 0$) while transport is ensured at leading order by non-zero vertical fluxes $\overline{w'X'}$ which may even be up-gradient. Indeed, using the assumption of a mixed-layer $\partial_z \overline{X} \simeq 0$ into a turbulent transport equation of the type $\partial_t \overline{X} + \partial_z \overline{w'X'} = 0$ implies that $\overline{w'X'}$ varies linearly with z. Such linear variation of fluxes in the mixed layer is well-supported by observations and numerical experiments (Garratt, 1994; Denbo & Skyllingstad, 1996).

To circumvent ED hypothesis, Deardorff (1966) proposed to introduce a constant non-local term γ_X in the form $\overline{w'X'} = -K_X(\partial_z \overline{X} - \gamma_X)$. Later on, such a formulation has been refined, where both K_X and γ_X were prescribed by a self-similar profile function depending on external characteristics of the boundary layer such as surface forcing, stratification at the atmospheric top (or oceanic base) of the mixed layer and implicitly defined mixed layer height (see Troen and Mahrt (1986); Holtslag and Moeng (1991) for atmospheric models, Large et al. (1994) for oceanic models). This approach is still in use in some present-day ocean models (e.g. via the CVMIX library, Van Roekel et al., 2018). Furthermore two other types of convective parameterization are sometimes used: (*i*) a buoyancy sorting scheme (a.k.a. adjustment scheme or non-penetrative scheme), in which static instabilities are eliminated in one time-step by mixing downward neighboring vertical levels until a neutral buoyancy profile is attained (e.g. Madec et al., 1991) (*ii*) an enhanced eddy-viscosity scheme in which the vertical diffusivity coefficient is artificially increased to a high value as soon as static instabilities are found on the density profiles (Madec et al., 2019). These two approaches are ad-hoc and cannot be derived from first principles.

The present work builds on the combined Eddy-Diffusivity and Mass-Flux (EDMF) parameterization schemes (Hourdin et al., 2002; Soares et al., 2004). The ED component aims to represent turbulent transport in a nearly isotropic environment, in which convective plumes -modeled by MF terms- support a non-local advective transport. The MF concept was originally introduced in the atmospheric context to represent deep convective clouds (Arakawa & Schubert, 1974), then it has been adapted to represent shallow and dry boundary layer convection in combination with ED schemes. It is intrinsically based on a multi-fluid averaging (Yano, 2014; Thuburn et al., 2018) of the fluid equations. In ocean models the EDMF concept has been first introduced by Giordani et al. (2020), and has been gaining increasing attention (e.g. Garanaik et al. (2024), or a recent implementation in the code Oceananigans, Ramadhan et al. (2020)).

1.2 Parameterization development and physics dynamics coupling

The general objective of the proposed work is to approach the parameterization problem in a "consistent" manner. Here the notion of consistency integrates various aspects: consistent dynamical and thermodynamical approximations between resolved and subgrid models, energetic consistency at both continuous (e.g. Eden, 2016; Jansen et al.,

2019; Eden & Olbers, 2014) and discrete (e.g. Burchard, 2002) levels, consistency with a particular choice of scale-separation operator (Higgins et al., 2013; Lauritzen et al., 2022), and the rigorous reduction of a physical system to a scale-aware parametric representation based on well-identified approximations and hypotheses (Honnert et al., 2016; Tan et al., 2018).

Regarding boundary layer parameterizations, turbulent kinetic energy (TKE) or its budget can serve to compute viscous dissipation, which is key to close the total energy budget. Moreover some schemes use prognostic TKE to scale the intensity of eddy-diffusivity. By using energy arguments, we aim to remove ambiguity around three practical topics: how to interpret TKE in the model; whether to use ED or EDMF fluxes in the source terms of TKE; what are consistent boundary conditions? The question of the fluxes appears ambiguous in the litterature. Some studies use ED fluxes (Giordani et al., 2020; Hourdin et al., 2019; Han et al., 2016). Other studies use explicitly the full EDMF fluxes (Han & Bretherton, 2019; Witek et al., 2011). However the majority of studies and documentations are ambiguous or not explicit about this point, and modelling choices are often motivated by simulation outputs rather than consistency. In this paper, we argue that energy conservation constraints can guide without ambiguity such choices. TKE represents a subgrid kinetic energy that exchanges energy with the resolved reservoirs. The use of mass-flux terms leads to energy transfers and redistributions that must be taken into account in the TKE equation to ensure energetic consistency between resolved and subgrid scales. In addition, the boundary conditions of the mass-flux equations must be consistent between ED and MF to avoid double-counting and subsequent artificial energy fluxes at the fluid boundary.

The aim of this paper is two-fold. First, we intend to provide an introductory, self-contained, and pedagogical derivation of EDMF schemes starting from first principles, to guide consistency considerations. Second, we derive theoretical energy budgets and provide guidelines to obtain energetically consistent EDMF models. Consequently, this paper is intended to both the oceanographic community as a comprehensive introduction to EDMF, and the atmospheric community seeking to reduce energy biases in EDMF models.

1.3 Organization of the paper

The paper is organized as follows. In section 2, we expose the derivation of an EDMF scheme from first principle, systematically discuss the successive assumptions at stake, provide closures according to state-of-the-art practice, and discuss consistent boundary conditions. In section 3, we recall the theoretical closure-agnostic resolved and subgrid energy budgets of a horizontally averaged anelastic (or Boussinesq) fluid, including radiative heating. In section 4, we expose analogous energy budgets when using an EDMF closure, including consistent TKE equation, and propose a new formulation for TKE transport. Furthermore, we derive vertically averaged energy budgets to reveal the net contribution of shear and the role of boundary conditions on the energy fluxes. In a companion paper (Perrot and Lemarié (2024); hereafter Part II) we assess the validity of hypotheses and the sensitivity of the scheme to modelling choices against Large Eddy Simulations (LES) and observational data of oceanic convection, detail an energy-conserving discretization, and quantify energy biases of inconsistent formulations.

2 Derivation of EDMF scheme

2.1 Formal derivation

We start from the unaveraged anelastic non-hydrostatic system in conservative form (e.g. eq. (76-80) of Tailleux & Dubos, 2024) in a cubic domain $L_x \times L_y \times H$, describ-

ing either a dry atmosphere or a salty ocean:

$$\partial_t \boldsymbol{u} = -\frac{1}{\rho_R}\nabla\cdot(\rho_R \boldsymbol{u}\otimes\boldsymbol{u}) - \nabla\left(\frac{p^\dagger}{\rho_R(z)}\right) + b\boldsymbol{e}_z + \frac{1}{\rho_R}\nabla\cdot(\rho_R\boldsymbol{\tau}) \tag{1}$$

$$\nabla\cdot(\rho_R(z)\boldsymbol{u}) = 0 \tag{2}$$

$$\partial_t \theta = -\frac{1}{\rho_R}\nabla\cdot(\rho_R\boldsymbol{u}\theta) + P_\theta \tag{3}$$

$$\partial_t S = -\frac{1}{\rho_R}\nabla\cdot(\rho_R\boldsymbol{u}S) \tag{4}$$

$$b = -g\frac{\rho_{\rm EOS}-\rho_R(z)}{\rho_{\rm EOS}} \tag{5}$$

$$\rho_{\rm EOS} = \rho_{\rm EOS}(\theta, S, p_R(z)) \tag{6}$$

where $\boldsymbol{u}=(u,v,w)$ denotes the velocity field in a local Cartesian frame of reference $(\boldsymbol{e}_x,\boldsymbol{e}_y,\boldsymbol{e}_z)$, z ranges from 0 to H in the atmosphere and $-H$ to 0 in the ocean, $\rho_R(z)$ is a reference density profile, the pressure has been decomposed as $p=p_R(z)+p^\dagger(x,y,z,t)$ with $\partial_z p_R = -\rho_R g$, b is the buoyancy acceleration, θ is potential temperature, S is the mass concentration of an additional component of the fluid (in kg/kg; typically salt in the ocean or any passive tracer in the atmosphere), P_θ is an additional source of potential temperature that will be specified in E3 via energy constraints, $\boldsymbol{\tau}=\nu 1/2(\nabla\boldsymbol{u}+\nabla\boldsymbol{u}^T)$ is the viscous stress tensor.

Remark that by specifiying $\rho_R(z) = \rho_0 = \text{cst}$, we obtain a Boussinesq system with buoyancy given by (5) instead of the more traditional form $-g(\rho_{\rm EOS}-\rho_0)/\rho_0$ (Tailleux & Dubos, 2024; Eldred & Gay-Balmaz, 2021). This so-called Boussinesq-anelastic formulation has the advantage to possess "potential energy and thermodynamic potentials that are nearly identical to their exact counterparts so that their energetics is more easily comparable to that of the fully compressible equations and do not require the introduction of artificial and ad-hoc thermodynamic potentials" (Tailleux & Dubos, 2024). For simplicity, we restrict to the case of a dry atmosphere and of seawater with a linearized equation of state[1]. Moreover we do not include the Coriolis term in the present study. Since the Coriolis force is energetically-neutral it does not interfere with the derivations made throughout this paper.

Next, we detail the framework in which vertical mixing parameterizations are usually developed. We adopt a semi-discrete description, where the horizontal fluid domain is *discretized* into a $N_x\times N_y$ mesh whereas time and vertical coordinates z are kept as *continuous* variables. Each horizontal grid cell has length Δx_i and width Δy_j ($i=1,\dots,N_x$; $j=1,\dots,N_y$), and we denote (x_i,y_j) its center. The spatial domain can be thought of $N_x\times N_y$ vertical columns stacked together. In a numerical model discretized on such a mesh, the computed variables would be interpreted in a finite volume approach (LeVeque, 2002): for any field $X=\boldsymbol{u},\theta,S...$ one can define the following horizontal average and fluctuation

$$\overline{X}(x_i,y_j,z,t) := \frac{1}{\Delta x_i\Delta y_j}\int_{\Delta x_i\times\Delta y_j} X(x,y,z,t)\,\mathrm{d}x\mathrm{d}y, \qquad X' = X-\overline{X}$$

If we recast (1)–(6) in the generic form $\partial_t X + \frac{1}{\rho_R}\nabla\cdot(\rho_R\boldsymbol{u}X) = P_X$, and then apply such a horizontal average, we obtain

$$\partial_t\overline{X} + \frac{1}{\rho_R}\partial_z\left(\rho_R\overline{w}\,\overline{X} + \rho_R\overline{w'X'}\right) + \frac{1}{\Delta x_i\Delta y_j}\oint_{\partial(\Delta x_i\times\Delta y_j)} X\boldsymbol{u}_h\cdot\mathrm{d}\boldsymbol{n} = \overline{P}_X \tag{7}$$

[1] In both oceanic and atmospheric context, we use simple thermodynamic descriptions allowing convection. Although these descriptions are inaccurate for real-world applications, they are sufficient to expose how to build energetically consistent EDMF parameterizations.

where $\boldsymbol{u}_h = (u, v, 0)$ denotes the horizontal velocity vector and $\mathrm{d}\boldsymbol{n}$ is an outward pointing line integral element, i.e. $\boldsymbol{u}_h \cdot \mathrm{d}\boldsymbol{n} = u\mathrm{d}y - v\mathrm{d}x$. In a numerical model, $\overline{X}$ would be interpreted as the resolved variable, X' would be an unresolved fluctuation, the boundary integral in (7) would be interpreted as the divergence of the total (resolved and subgrid) horizontal flux of X (precise form of the horizontal flux would depend on the numerical scheme and possibly on parameterizations), and the vertical subgrid flux $\overline{w'X'}$ has to be closed via a parameterization.

When focusing on the parameterization of vertical mixing processes, it is common to conceptually isolate one vertical column of fluid to work with a one-dimensional Single-Column Model (SCM) (e.g. Zhang et al., 2016). Any quantity is assumed statistically invariant along the horizontal direction, meaning that in practice the horizontal fluxes and pressure gradients are neglected. We further simplify the problem with two additional assumptions: First, the bottom (or top for the ocean) of the column is considered flat. Along with a non-penetration condition, this leads to $\overline{w}(z=0) = 0$. Now the horizontal homogeneity assumption implies that $\overline{\partial_x(\rho_R u) + \partial_y(\rho_R v)} = 0$, thus mass conservation reads $\partial_z(\rho_R \overline{w}) = 0$. Along with the non penetration condition it implies $\overline{w}(z) = 0$ at any level z. Second, in the vertical momentum budget, the momentum flux divergence $\partial_z \overline{w'w'}$ is neglected, leading to the hydrostatic approximation $\partial_z \overline{p}^\dagger = b$. The resulting SCM equations are then

$$\partial_t \overline{\boldsymbol{u}}_h = -\frac{1}{\rho_R}\partial_z(\rho_R \overline{w'\boldsymbol{u}'_h}) \tag{8}$$

$$\partial_t \overline{\theta} = -\frac{1}{\rho_R}\partial_z(\rho_R \overline{w'\theta'}) + \overline{P}_\theta \tag{9}$$

$$\partial_t \overline{S} = -\frac{1}{\rho_R}\partial_z(\rho_R \overline{w'S'}) \tag{10}$$

where the molecular viscosity can be safely neglected in the mean momentum budget. The remainder of this article will use these SCM assumptions, and indices i, j will be dropped. For readers interested in the inclusion of horizontal fluxes, we refer them to Yano (2014) and Tan et al. (2018). As an alternative to the semi-discrete description presented above, a fully continuous description can be carried out by replacing the horizontal average by smoothing kernels on the scale of the grid size (see for example Thuburn et al. (2018) in the context of mass-flux schemes).

We now *assume* a formal decomposition of the horizontal column area $\Delta x \times \Delta y$ into two horizontal subdomains of areas $\mathcal{A}_e(z,t)$ and $\mathcal{A}_p(z,t)$ which also depend on depth and time (see fig. 1). Such decomposition is meant to isolate the coherent convective structures usually referred to as *plumes* (occupying the subdomain of area $\mathcal{A}_p(z,t)$) from the rest of the flow, referred to as the *environment* (occupying the subdomain of area $\mathcal{A}_e(z,t)$). We introduce the following notations to characterize the subdomain averaged fields, fluctuations and *fractional* area ($i = e$ for environmental variables and $i = p$ for plume variables):

$$X_i = \frac{1}{\mathcal{A}_i(z,t)} \int_{\mathcal{A}_i(z,t)} X(x,y,z,t)\,\mathrm{d}x\mathrm{d}y, \qquad X'_i = X - X_i$$
$$a_i = \mathcal{A}_i(z,t)/(\Delta x \times \Delta y)$$

Any mean field can then be decomposed as

$$\overline{X} = a_e X_e + a_p X_p$$

In particular, when $X \equiv 1$ we get the constraint $a_e = 1 - a_p$. After some algebra, any turbulent flux can be recast as

$$\overline{w'X'} = a_e \overline{w'_e X'_e} + a_p \overline{w'_p X'_p} + a_e(w_e - \overline{w})(X_e - \overline{X}) + a_p(w_p - \overline{w})(X_p - \overline{X}) \tag{11}$$

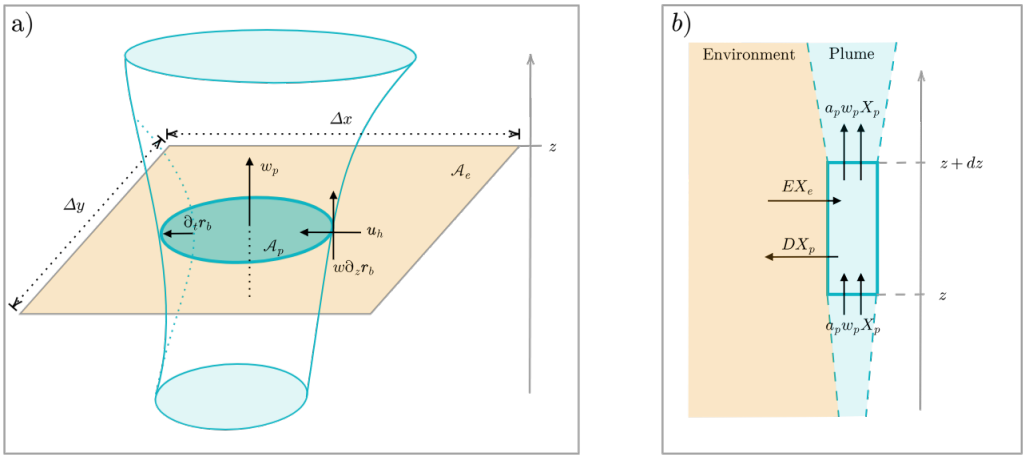

Figure 1: Schematic of representation of: (a) a 3D plume (blue volume) embedded into the environment. At a given level z, horizontal grid cell $\Delta x \times \Delta y$ is decomposed into plume area $\mathcal{A}_p$ (blue shading) and environment area $\mathcal{A}_e$ (orange shading). Fluxes of fluid and tracers across the boundary $\partial\mathcal{A}_p$ are due to horizontal velocity across the boundary $\boldsymbol{u}_h$, to (apparent) horizontal velocity of the boundary $\partial_t \boldsymbol{r}_b$ and to vertical velocity if the boundary of the 3D plume is vertically tilted ($\partial_z \boldsymbol{r}_b \neq 0$). (b) Horizontal and vertical fluxes of tracer X into the equivalent "single" plume, within the upstream approximation. See text for details.

where

$$\overline{w_i' X_i'} = \frac{1}{\mathcal{A}_i(z,t)} \int_{\mathcal{A}_i(z,t)} (X - X_i)(w - w_i)\,\mathrm{d}x\mathrm{d}y$$

Here we kept $\overline{w}$ for generality, however as explained above the horizontal homogeneity assumption implies $\overline{w} = 0$. For each subdomain, the $a_i(w_i - \overline{w})(X_i - \overline{X})$ terms in (11) account for the "mass-flux" (i.e. the contribution of coherent structures to the flux), whereas the $a_i \overline{w_i' X_i'}$ terms are a contribution from internal variability within subdomain i. Applying the subdomain average to any conservation law of the form $\partial_t X + \frac{1}{\rho_R}\nabla\cdot(\rho_R \boldsymbol{u} X) = P_X$ and using Reynolds transport theorem leads to (see appendix A of Tan et al. (2018) and Yano (2014) for full derivation)

$$\partial_t(a_i X_i) + \frac{1}{\rho_R}\partial_z\left(\rho_R a_i w_i X_i + \rho_R a_i \overline{w_i' X_i'}\right) + \frac{1}{\mathcal{A}_i}\oint_{\partial\mathcal{A}_i} X \boldsymbol{u}_r \cdot \mathrm{d}\boldsymbol{n} = a_i P_{X,i} \tag{12}$$

where the relative horizontal boundary velocity is $\boldsymbol{u}_r = \boldsymbol{u}_h - \partial_t \boldsymbol{r}_b - w\partial_z \boldsymbol{r}_b$ and $\boldsymbol{r}_b = (x_b(z,t), y_b(z,t))$ is the position vector of boundary elements. The three terms that constitute $\boldsymbol{u}_r$ indicate that boundary fluxes can arise respectively due to horizontal velocity across the boundary, to (apparent) horizontal velocity of the boundary, or to vertical velocity if the boundary of the 3D plume is vertically tilted (i.e. $\partial_z \boldsymbol{r}_b \neq 0$; see fig. 1(a)).

2.2 Standard assumptions

2.2.1 Plume-Environment decomposition

The first standard assumption we have already made is to consider only two subdomains, the convective plume and the environment. This is justified since in convective situations the main contribution to the fluxes comes from the plumes. However, the framework is flexible enough to incorporate an arbitrary number of components, such

as multiple updrafts or downdrafts. In particular, several studies of the atmospheric convective boundary layer (CBL) underline the importance of returning coherent structures around the plumes, often referred to as CBL downdrafts (Schmidt & Schumann, 1989; Couvreux et al., 2007; Brient et al., 2023).

2.2.2 Entrainment/Detrainment and Upstream approximation

Net fluid exchange at the horizontal boundary of the plume domain can be further decomposed into fluid *entrained* into the plume from the environment, and fluid *detrained* out of the plume into the environment, namely

$$\begin{aligned}\frac{1}{\mathcal{A}_p}\oint_{\partial\mathcal{A}_p}\boldsymbol{u}_r\cdot\mathrm{d}\boldsymbol{n} &= \frac{1}{\mathcal{A}_p}\oint_{\partial\mathcal{A}_p,\boldsymbol{u}_r>0}\boldsymbol{u}_r\cdot\mathrm{d}\boldsymbol{n}+\frac{1}{\mathcal{A}_p}\oint_{\partial\mathcal{A}_p,\boldsymbol{u}_r<0}\boldsymbol{u}_r\cdot\mathrm{d}\boldsymbol{n}\\ &= D-E\end{aligned}$$

where $E(>0)$ is called *entrainment rate* and $D(>0)$ is called *detrainment rate*. We further assume that the value of X at the boundary is either equal to the mean value in the environment when entrainment is occurring, or the mean value in the plume when detrainment is occurring. This is the so-called *upstream approximation*, formulated as[2]

$$\frac{1}{\mathcal{A}_p}\oint_{\partial\mathcal{A}_p}X\boldsymbol{u}_r\cdot\mathrm{d}\boldsymbol{n}=X_eE-X_pD \tag{13}$$

As a result of this approximation, the plume equation reads (fig. 1(b))

$$\partial_t(a_pX_p)+\frac{1}{\rho_R}\partial_z(\rho_Ra_pw_pX_p)=-\frac{1}{\rho_R}\partial_z(\rho_Ra_p\overline{w_p'X_p'})+EX_e-DX_p+a_pP_{X,p} \tag{14}$$

In particular when $X\equiv 1$, we get the plume area conservation equation:

$$\partial_ta_p+\frac{1}{\rho_R}\partial_z(\rho_Ra_pw_p)=E-D \tag{15}$$

from which we can rewrite the plume equation in advective form,

$$a_p\partial_tX_p+a_pw_p\partial_zX_p=-\frac{1}{\rho_R}\partial_z(\rho_Ra_p\overline{w_p'X_p'})+E(X_e-X_p)+a_pP_{X,p} \tag{16}$$

2.2.3 Steady plume hypothesis

A common hypothesis is that the plume domain is in a quasi-steady regime, thus neglecting the temporal tendency compared to vertical advection. The relevance of this hypothesis is numerically tested in idealized LES cases in Part II. An *a priori* scaling estimation can also be performed. Let h be the boundary layer depth, which can also serve as a length scale for the mean plume. A characteristic time scale for the mean plume is $\tau_p=h/W$ where W is a plume vertical velocity scale. A time scale associated to the boundary layer growth and mean fields evolution is $\tau_{\mathrm{BL}}=h/w_{\mathrm{ent}}$ where $w_{\mathrm{ent}}=\mathrm{d}h/\mathrm{d}t$ is the boundary layer vertical entrainment velocity. In the limit of free convection triggered by a surface buoyancy loss $B_0<0$ into a fluid of constant stratification N_0^2, the classical convective scalings $h\propto\sqrt{(-B_0/N_0^2)t}$ and $W=w_*=(-B_0h)^{1/3}$ (Turner, 1979; Deardorff, 1970) leads to

$$\frac{\tau_p}{\tau_{\mathrm{BL}}}=\frac{w_{\mathrm{ent}}}{W}\propto\frac{1}{(N_0t)^{2/3}} \tag{17}$$

[2] In the context of 3D models, the plume boundary $\partial\mathcal{A}_p$ can cross the horizontal boundary of the grid cell. The corresponding contribution to the integral can be interpreted as a resolved flux divergence across the grid cell, namely $\nabla_h\cdot(a_p\boldsymbol{u}_{h,p}X_p+a_p\overline{\boldsymbol{u}_{h,p}'X_p'})$ (see section 5.1 of Yano (2014)).

In a different context, that of the development of a shear-driven mixed layer forced by surface wind stress $\rho_0 u_*^2$, Kato and Phillips (1969) showed that $w_{\text{ent}}/u_* \propto u_*^2/N_0^2 h$. In such a layer $W \simeq u_*$, leading to a scaling similar to (17). These scalings suggest that as long as the surface forcings (represented here by u_* and B_0) are evolving slowly compared to $1/N_0$, the steady plume hypothesis remains valid. Under such a hypothesis, the plume equation for any field X and the plume area conservation now read

$$\frac{1}{\rho_R}\partial_z(\rho_R a_p w_p X_p) = -\frac{1}{\rho_R}\partial_z(\rho_R a_p \overline{w_p' X_p'}) + E X_e - D X_p + a_p P_{X,p} \tag{18}$$

$$\partial_z(\rho_R a_p w_p X_p) = E - D \tag{19}$$

As a summary, we rewrite the coupled resolved/plume system in an advective form using area conservation and $\overline{X} = (1-a_p)X_e + a_p X_p$ and the identity $(X_e - \overline{X}) = \frac{-a_p}{1-a_p}(X_p - \overline{X})$ (a summary of useful identities can be found in Appendix A):

$$\partial_t \overline{X} = -\frac{1}{\rho_R}\partial_z(\rho_R \overline{w' X'}) + \overline{P}_X \tag{20}$$

$$\overline{w' X'} = \frac{1}{1-a_p} a_p w_p (X_p - \overline{X}) + (1-a_p)\overline{w_e' X_e'} + a_p \overline{w_p' X_p'} \tag{21}$$

$$a_p w_p \partial_z X_p = -\frac{1}{1-a_p} E (X_p - \overline{X}) - \frac{1}{\rho_R}\partial_z(\rho_R a_p \overline{w_p' X_p'}) + a_p P_{X,p} \tag{22}$$

Several authors have recently proposed to relax the steady plume hypothesis (Tan et al., 2018; Thuburn et al., 2018). However, the overwhelming majority of mass flux schemes implemented in realistic models considers a plume domain in a quasi-steady regime.

2.2.4 Small area limit

A last standard hypothesis is that the fractional area of the plume is *small* compared to that of the environment (see Part II for a direct evaluation against LES). This generally means considering the formal limit $a_p \to 0$ and $a_e \to 1$ in the previous equations while keeping non-zero mass-flux $a_p w_p$ and source terms. Yano (2014) proposes to assume $a_p w_p = O(w_e)$ and $a_p P_{X,p} = O(S_{X,e})$ to retain an order one contribution of $a_p w_p (X_p - \overline{X})$ in (21), to neglect subplume fluxes $\overline{w_p' X_p'}$ and to keep an order one contribution of advection and forcings in (22). In the small area limit, any environmental field X_e (except w_e) can be approximated by the mean field, the vertical turbulent flux (21) becomes

$$\overline{w' X'} = a_p w_p (X_p - \overline{X}) + \overline{w_e' X_e'} \tag{23}$$

and the plume equation (22) now reads

$$a_p w_p \partial_z X_p = -E(X_p - \overline{X}) + a_p P_{X,p} \tag{24}$$

In the remainder of this study, we will adopt such a small area limit. Noteworthy is the effort by some authors to relax this hypothesis to explore the "grey zone" of atmospheric turbulence or to devise scale-aware parameterization schemes when the grid is refined to the point where a_p is no longer small (Honnert et al., 2016; Tan et al., 2018). For the sake of completeness, we include in Appendix B the system of plume equations obtained when relaxing the small area limit while still neglecting subplume fluxes $\overline{w_p' X_p'}$ (in line with Tan et al. (2018)). This system only deviates by factors $1/(1-a_p)$ from the "small-area" system, making it simple to implement in practice.

2.3 Standard Closures

Thanks to the assumptions made so far, we have arrived at equations of the general form (24) for the plume, and (23) for vertical turbulent fluxes. At this stage, additional closure assumptions are required to express the entrainment and detrainment rates, the flux $\overline{w_e' X_e'}$, and the pressure gradients appearing in the $P_{w,p}$ and $P_{\boldsymbol{u}_h,p}$ terms.

2.3.1 Plume vertical pressure gradient

Plume vertical pressure gradients are usually parameterized as the combination of a virtual mass term (e.g. Bretherton et al., 2004) – representing the reduction of plume buoyancy due to pushing and pulling on the environment –, a reduced entrainment term and a quadratic drag term (Simpson & Wiggert, 1969; Romps & Charn, 2015). Several formulations have been proposed (see Roode et al. (2012) for an intercomparison in the context of shallow cumulus convection). Alternatively several authors point out the importance of non-local (in height) effects (Peters, 2016; Kuo & Neelin, 2022), leading to recent formulations on e.g. velocity divergence (Weller et al., 2020), or adaptive updraft radius (He et al., 2021; Peters et al., 2021). A detailed intercomparison of these different closures is out of the scope of this paper. Here we adapt some usual practices in the atmospheric context (e.g. Pergaud et al., 2009; Rio et al., 2010) and consider

$$-a_p \left(\partial_z(p^\dagger/\rho_R)\right)_p \quad = \quad (a-1)a_p B_p + (b-1)(-Ew_p) + b'\frac{1}{h}a_p w_p^2 \tag{25}$$

leading to the plume vertical momentum budget

$$a_p w_p \partial_z w_p \quad = \quad a a_p B_p - bEw_p - \sigma_o^a b'\frac{1}{h}a_p w_p^2 \tag{26}$$

where a, b and b' are positive non-dimensional parameters, $\sigma_o^a = +1$ in the atmosphere and -1 in the ocean, and $B_p = b_p - \overline{b}$. The plume vertical extent $h = h(t)$ is computed as the height (or depth) at which the plume vertical velocity w_p goes to zero. Since plumes are structures of aspect ratio close to 1, h provides an acceptable scale to substitute the constant plume radius classically used in the drag term (Simpson & Wiggert, 1969; Romps & Charn, 2015; Tan et al., 2018; Weller et al., 2020). The main advantage of our formulation is to avoid the introduction of a constant *dimensional* radius coefficient which would restrict parameterization universality. Note that in the case of dry atmosphere or seawater with a linearized equation of state, we have $b_p - \overline{b} = b_{\rm eos}(\theta_p, S_p, p_R(z)) - b_{\rm eos}(\overline{\theta}, \overline{S}, p_R(z))$.

2.3.2 Horizontal momentum budget

Based on the work of Rotunno and Klemp (1982) and Wu and Yanai (1994), Gregory et al. (1997) proposed a parameterization of the plume horizontal pressure gradient as an advective correction of the form

$$-a_p \left(\nabla_h \frac{p^\dagger}{\rho_R}\right)_p = a_p w_p C_u \partial_z \overline{\boldsymbol{u}}_h \tag{27}$$

where C_u is a parameter. It imposes a relaxation of the plume shear towards the grid-scale shear. We show in Section 4.4 that energy constraints impose $0 \leq C_u < 1$.

2.3.3 Eddy-Diffusivity closure

The environment is thought of as a subdomain where only small-scale turbulence occurs, thus supporting the hypothesis of a closure of the vertical flux with an eddy-diffusivity, $\overline{w'_e X'_e} \underset{\rm ED}{=} -K_X \partial_z X_e \underset{a_p \ll 1}{\simeq} -K_X \partial_z \overline{X}$. This leads to the eddy-diffusivity mass-flux closure of subgrid fluxes

$$\overline{w'X'} = \underbrace{-K_X \partial_z \overline{X}}_{\rm ED} + \underbrace{a_p w_p (X_p - \overline{X})}_{\rm MF} \tag{28}$$

In order to compute the eddy-diffusivity coefficient K_X, various approaches relying either on self-similar empirical profiles (e.g. Siebesma et al., 2007; Han et al., 2016) or on prognostic turbulent kinetic energy (e.g. Hourdin et al., 2019) can be found in the litterature. However the practical choice of a closure do not directly affect energy budgets of the SCM.

$\overline{w'\theta'}$	$= a_p w_p(\theta_p - \overline{\theta}) - K_\theta \partial_z \overline{\theta}$	Vertical turbulent flux of temperature
$\overline{w'S'}$	$= a_p w_p(S_p - \overline{S}) - K_S \partial_z \overline{S}$	Vertical turbulent flux of component S
$\overline{w'\boldsymbol{u}'_h}$	$= a_p w_p(\boldsymbol{u}_{h,p} - \overline{\boldsymbol{u}}_h) - K_u \partial_z \overline{\boldsymbol{u}}_h$	Vertical turbulent momentum flux
$\partial_z(a_p w_p)$	$= E - D$	Plume area conservation equation
$a_p w_p \partial_z \phi_p$	$= E(\overline{\phi} - \phi_p) + P_{\phi,p}$	Plume equation for component $\phi = \theta, S$
$a_p w_p \partial_z \boldsymbol{u}_{h,p}$	$= E(\overline{\boldsymbol{u}}_h - \boldsymbol{u}_{h,p}) + a_p w_p C_u \partial_z \overline{\boldsymbol{u}}_h$	Plume horizontal momentum equation
$a_p w_p \partial_z w_p$	$= -bE w_p + a_p \left\{ a B_p - \sigma_o^a b' (w_p)^2 \right\}$	Plume vertical velocity equation
B_p	$= b_{\text{eos}}(\phi_p) - b_{\text{eos}}(\overline{\phi})$	Buoyancy forcing term
K_u	$= c_m l_m \sqrt{k}$	Eddy-viscosity
$K_S = K_\theta$	$= K_u \left(\text{Pr}_t\right)^{-1}$	Eddy-diffusivity

Table 1: Summary of the vertical turbulent flux formulation and plume equations in the small area limit under the steady plume hypothesis detailed in sections 2.1, 2.2 and 2.3.

2.3.4 Entrainment and detrainment closures

Entrainment and detrainment closures are still a topic of extensive research in the atmospheric modeling community. One difficulty is that a given closure can only be specific to a certain type of convection (de Rooy et al., 2013). To close entrainment and detrainment rates[3], we adapt the formulation proposed by Rio et al. (2010), namely

$$E = a_p \beta_1 \max(0, \partial_z w_p) \tag{29}$$

$$D = -a_p \beta_2 \min(0, \partial_z w_p) + \sigma_o^a a_p w_p \frac{\delta_0}{h} \tag{30}$$

where the two parameters β_1 and β_2 are positive, δ_0/h is a positive minimum detrainment (some authors also include a minimum "turbulent" entrainment, e.g. Cohen et al. (2020)).

To summarize the formal derivation made so far, the closure of fluxes and associated plume equations of the resulting EDMF scheme are provided in Tab. 1.

2.4 Consistent boundary conditions for mean and plume equations

2.4.1 General concepts

Under the aforementioned assumptions, the budget equations governing plume quantities simplify into a system of non-linear first-order ordinary differential equations with respect to the variable z. Accordingly, a single boundary condition at $z = 0$ (i.e., the top of the water column or the bottom of the air column depending on the fluid under consideration) is sufficient for the computation of plume variables. At the boundary $z = 0$, consistent boundary conditions for the plume variable X_p and the mean variable $\overline{X}$ must comply with the EDMF flux decomposition (28)

$$\overline{w'X'}(0) = -K_X \partial_z \overline{X}(0) + a_p(0) w_p(0) (X_p(0) - \overline{X}(0)) \tag{31}$$

[3] In the literature, closures are usually provided for *fractional* entrainment and detrainment rates, respectively $\epsilon = E/(\sigma_o^a a_p w_p)$ and $\delta = D/(\sigma_o^a a_p w_p)$, where $-a_p w_p$ is the oceanic mass-flux for downdrafts and $+a_p w_p$ is the atmospheric mass-flux for updrafts.

Such a constraint should guide modeling choices concerning boundary conditions. Indeed, it systematically guarantees the correct partition of surface fluxes, and thus avoids double-counting biases linked to non-physical energy sources/sinks at the boundary (see Sec. 4.2). For instance, suppose the values of $\overline{w'X'}(0)$, $a_p(0)$, $w_p(0)$ and $X_p(0)$ are jointly specified. Then (31) would turn into a Robin (a.k.a type 3) boundary condition for the $\overline{X}$ equation which arises naturally in advection-diffusion equations (e.g. Hahn and Özişik (2012), chapter 1-5). At the boundary $z = \sigma_o^a H$, a no-flux condition is imposed for the mean equation. For the specific case of oceanic convection reaching the ocean bottom, a possibility is to add a penalization term nudging the solution towards the condition $w_p(z = -H) = 0$.

2.4.2 Oceanic context

For oceanographic applications, we consider that a surface flux $\overline{w'X'}(0)$ is prescribed. The mass flux component becomes non-zero close to the surface as soon as the plume is accelerating and entrainment rate (29) is itself non-zero. For simplicity we consider here $\delta_0 = 0$. In this case the conservation of volume reads

$$\partial_z(a_p w_p) = a_p w_p \left(\beta_1 \frac{1}{w_p}\partial_z w_p\right)$$

which can be easily integrated vertically to obtain

$$a_p(z)w_p(z) = (a_p(0)w_p(0)) \left(\left(\frac{w_p(z)}{w_p(0)}\right)^{\beta_1}\right)$$

Except fot singular case $\beta_1 = 1$, non-trivial solutions are obtained if and only if non-zero boundary values for a_p and w_p are chosen. In the remainder, we adopt the following simple choice,

$$X_p(0) = \overline{X}(0),\ a_p(0) = a_p^0,\ w_p(0) = w_p^0$$

where a_p^0 and w_p^0 are parameters. According to (31), it implies that all the surface flux is allocated in the ED component, as advocated by Tan et al. (2018). This particular choice of boundary condition is also motivated by the fact that it implies that convection is triggered as soon as the surface Brünt-Väisälä frequency $\partial_z b(0)$ is negative (see Appendix C for further details). As a result, (31) turns into the Neumann boundary condition $-K_X \partial_z X(0) = \overline{w'X'}(0)$, which is standard practice for ED-only closures.

Alternatively, Soares et al. (2004) proposed that close to the surface, the plume/mean temperature difference should depend on the surface heat flux, leading to

$$\theta_p(z) = \overline{\theta}(z) + \beta \frac{\overline{w'\theta'}(0)}{\sqrt{k}(z)} \tag{32}$$

where β is a constant. We show in Appendix C that our formulation is in fact equivalent to (32) for if $\beta = z/(c_b l_b(0))$ and $k(z) \simeq k(0)$ (where c_b is a constant and l_b a mixing length associated to buoyancy). Thus our simple choice is equivalent to a forcing of the plume by surface buoyancy loss. However, when using this type of boundary condition exactly at the surface (as in Pergaud et al., 2009), the boundary condition for $\overline{\theta}$ must be modified in order to avoid double-counting of heat flux at the surface (see section 4.5).

2.4.3 Atmospheric context: consistency with Monin-Obukhov theory

For atmospheric applications, boundary conditions for the mean variables are commonly imposed using Monin-Obukhov similarity theory (MOST), which assumes that in a surface layer located between $z = 0$ and $z = z_1$ fluxes are constant, and mean variables obey a quasi-logarithmic profile. To properly include a surface layer obeying MOST,

then the EDMF flux decomposition must be imposed at the new model boundary $z = z_1$, namely

$$\overline{w'X'}(z_1) = -K_X(z_1)\partial_z\overline{X}(z_1) + a_p(z_1)w_p(z_1)(X_p(z_1) - \overline{X}(z_1)) \tag{33}$$

At this stage, we can point the following ambiguity. When the MF term is non-zero, it is not clear whether the flux arising from MOST – which is an ED flux – should be allocated to the ED term $-K_X(z_1)\partial_z\overline{X}(z_1)$, or to the total flux $\overline{w'X'}(z_1)$ using the constant flux assumption. Although not discussed transparently, it seems that the second option is a common practice. However, in such a case, special attention would be required to compute the total flux entering in energy budget computations.
Although beyond the scope of this article, we would like to point out that MOST is known to fail in strongly unstable conditions (Johansson et al., 2001; Li et al., 2018). Recently, Li et al. (2021) proposed corrections to formulate departure from MOST in the form of an EDMF closure including updraft *and* downdraft contributions. This approach could potentially help provide physically consistent boundary conditions to EDMF models.

At this stage, we have provided all the elements and underlying assumptions required to formulate an EDMF-type scheme (see Part II for the discretization aspects). Before studying the energetic impacts of using MF components, we derive theoretical horizontally averaged energy budgets.

3 Horizontally Averaged Energy Budgets

In this section, we derive horizontally averaged energy budgets regardless of flux parameterizations. As a starting point, we recall the closed energy budgets of the unaveraged anelastic system (or Boussinesq system if $\rho_R(z) = \rho_0$) derived for reference in Appendix E:

$$\begin{cases} \partial_t(\rho_R\mathcal{E}_k) + \nabla\cdot\left[\boldsymbol{u}\left(\rho_R E_k + p^\dagger\right) + \rho_R\nu\boldsymbol{u}\cdot\boldsymbol{\tau}\right] & = \rho_R wb - \rho_R\epsilon \\ \partial_t(\rho_R\mathcal{E}_i) + \nabla\cdot\left[\boldsymbol{u}\left(\rho_R\mathcal{E}_i + p_R\right)\right] + \nabla\cdot\left[\rho_R\boldsymbol{F}_\hbar\right] & = -\rho_R gw - \rho_R bw + \rho_R(\epsilon + \dot{q}_{\text{rad}}) \\ \partial_t(\rho_R\mathcal{E}_p) + \nabla\cdot\left[\boldsymbol{u}\rho_R\mathcal{E}_p\right] & = \rho_R gw \end{cases} \tag{34}$$

where the (unaveraged) total material energy has been divided into kinetic energy $\rho_R(z)\mathcal{E}_k = \rho_R(z)\frac{1}{2}\boldsymbol{u}\cdot\boldsymbol{u}$, internal energy $\rho_R\mathcal{E}_i = \rho_R(\hbar(\eta, S, p_R(z)) - p_R(z)/\rho_R(z))$ –whith $\hbar$ the specific enthalpy–, and potential energy $\rho_R\mathcal{E}_p = \rho_R gz$ (see e.g. Tailleux and Dubos (2024), where these authors referred to $\mathcal{E}_i + \mathcal{E}_p$ as "potential energy"). Moreover, the viscous stress tensor and viscous dissipation of kinetic energy have been written $\boldsymbol{\tau}$ and $\epsilon := -\nabla\boldsymbol{u} : \boldsymbol{\tau} = \nu\|\nabla\boldsymbol{u}\|^2$. $\boldsymbol{F}_\hbar$ is the (molecular) diffusive flux of enthalpy. The radiative heating $\dot{q}_{\text{rad}}$ is treated as an external energy source; consequently one would need to include the radiative energy $\mathcal{E}_r$ to the material energy in order to close the energy budget (see Appendix E for details).

Now, we will focus on the horizontal averages of these energies. First let us recall that the SCM assumptions (sec. 2.1) implies $\overline{w} = 0$. Then the averaged kinetic energy $\overline{\mathcal{E}_k}$ can be advantageously split into the kinetic energy of the horizontal resolved flow $E_k = (\overline{\boldsymbol{u}}_h\cdot\overline{\boldsymbol{u}}_h)/2$ (usually referred as *mean* or *resolved kinetic energy*) and the residual turbulent (or subgrid) kinetic energy $k = (\overline{\boldsymbol{u}'\cdot\boldsymbol{u}'})/2$. We will denote also by $E_{i+p} = \overline{\mathcal{E}_i + \mathcal{E}_p}$ the sum of averaged internal energy and potential energy. Upon averaging and applying the SCM assumptions, the budgets of the horizontally averaged energies E_k, k and E_{i+p} read

$$\begin{cases} \partial_t(\rho_R E_k) + \partial_z(\rho_R T_{E_k}) & = \rho_R\overline{w'\boldsymbol{u}'_h}\cdot\partial_z\overline{\boldsymbol{u}}_h \\ \partial_t(\rho_R k) + \partial_z(\rho_R T_k) & = -\rho_R\overline{w'\boldsymbol{u}'_h}\cdot\partial_z\overline{\boldsymbol{u}}_h + \rho_R\overline{w'b'} - \rho_R\overline{\epsilon} \\ \partial_t(\rho_R E_{i+p}) + \partial_z(\rho_R T_{E_{i+p}}) & = -\rho_R\overline{w'b'} + \rho_R(\overline{\epsilon} + \overline{\dot{q}}_{\text{rad}}) \end{cases} \tag{35}$$

and the transport terms that redistribute energy on the vertical are

$$\begin{cases} T_{E_k} & = \overline{w' \boldsymbol{u}_h'} \cdot \overline{\boldsymbol{u}}_h \\ T_k & = \overline{w' \frac{\boldsymbol{u}' \cdot \boldsymbol{u}'}{2}} + \frac{1}{\rho_R} \overline{w' p^{\dagger\prime}} - \nu \partial_z k \\ T_{E_{i+p}} & = \overline{w' \hbar'} \end{cases} \tag{36}$$

where we made the classical approximations that dissipation of mean KE is negligible, i.e. $\nu \|\nabla \overline{\boldsymbol{u}}\|^2 \simeq 0, \nu \overline{\|\nabla \boldsymbol{u}'\|^2} \simeq \overline{\epsilon}$ and neglected the (molecular) diffusive flux of enthalpy.

Now we are going to specify temperature equation, heat flux $\overline{w'\hbar'}$ and buoyancy flux $\overline{w'b'}$ for two fluids with simplified thermodynamics.

3.1 Dry atmosphere

For dry air in the anelastic approximation, specific enthalpy and buoyancy reads

$$\hbar(\theta, p_R(z)) = c_p T = c_p \theta \left(\frac{p_R(z)}{p_0} \right)^\kappa \tag{37}$$

$$b = -\partial_z(\hbar + gz) = g \frac{\theta - \theta_R(z)}{\theta_R(z)} \tag{38}$$

where c_p is a constant specific heat capacity of dry air, p_0 is a constant pressure reference, θ is the potential temperature, $\theta_R(z) = p_R \left(\frac{p_R(z)}{p_0} \right)^{-\kappa} / (\rho_R R_d)$ is the reference potential temperature profile, R_d is the specific dry air ideal constant, $\kappa = R_d/c_p$. We straightforwardly obtain an equation for the unaveraged potential temperature using the enthalpy budget (E13):

$$c_p \left(\frac{p_R}{p_0} \right)^\kappa \partial_t \theta + \frac{1}{\rho_R} \nabla \cdot \left(\rho_R c_p \left(\frac{p_R}{p_0} \right)^\kappa \theta \boldsymbol{u} + \rho_R \boldsymbol{F}_\hbar \right) = -gw - g \frac{\theta - \theta_R(z)}{\theta_R(z)} w + \epsilon + \dot{q}_{\text{rad}} \tag{39}$$

which can be rewritten after some algebra as

$$\partial_t \theta + \frac{1}{\rho_R} \nabla \cdot (\rho_R \theta \boldsymbol{u}) + \frac{1}{c_p} \left(\frac{p_R}{p_0} \right)^{-\kappa} \nabla \cdot (\rho_R \boldsymbol{F}_\hbar) = \frac{1}{c_p} \left(\frac{p_R}{p_0} \right)^{-\kappa} (\epsilon + \dot{q}_{\text{rad}}) \tag{40}$$

unveiling the advantage of working with potential temperature. The linearity of enthalpy with respect to θ allow to easily derive the following heat flux, buoyancy flux, internal and potential energy and mean temperature equation (again neglecting (molecular) diffusive fluxes),

$$\overline{w'\hbar'} = c_p \left(\frac{p_R}{p_0} \right)^\kappa \overline{w'\theta'}, \quad \overline{w'b'} = \frac{g}{\theta_R} \overline{w'\theta'}, \quad E_{i+p} = c_p \overline{\theta} \left(\frac{p_R}{p_0} \right)^\kappa - \frac{p_R}{\rho_R} + gz \tag{41}$$

$$\partial_t \overline{\theta} + \frac{1}{\rho_R} \partial_z (\rho_R \overline{w'\theta'}) = \frac{1}{c_p} \left(\frac{p_R}{p_0} \right)^{-\kappa} (\overline{\epsilon} + \overline{\dot{q}}_{\text{rad}}) \tag{42}$$

3.2 Boussinesq seawater with a linearized EOS

For seawater with a linearized EOS in Boussinesq approximation ($\rho_R(z) = \rho_0$) buoyancy reads

$$b = -\partial_z(\hbar + gz) = g\alpha(\theta - \theta_0) - \beta(S - S_0) \tag{43}$$

and a corresponding enthalpy can be formed as

$$\hbar(\theta, S, p_R(z)) = c_p \theta + \overbrace{\frac{p_R(z) - p_0}{\rho_0}}^{-gz} (1 + \alpha(\theta - \theta_0) - \beta(S - S_0)) \tag{44}$$

where c_p is a constant specific heat capacity of seawater, p_0 and ρ_0 are constant pressure and density references, α is the thermal expansion coefficient and β is the haline contracion coefficient. For a linearized equation of state potential and conservative temperature coincide, and they are denoted by θ. We show in appendix E32 that the unaveraged energetically consistent temperature equation is

$$\frac{D}{Dt}\theta = \frac{\epsilon + \dot{q}_{\text{rad}}}{c_p - \alpha g z} + \frac{-\nabla \cdot \boldsymbol{F}_{\hbar} + z g \beta \nabla \cdot \boldsymbol{F}_S}{c_p - \alpha g z} \tag{45}$$

where $\boldsymbol{F}_S$ is the (molecular) diffusive salt flux. The energy increase due to viscous dissipation is small and usually neglected in the ocean (e.g. McDougall, 2003; Olbers et al., 2012). In appendix E32 we show that by doing so it leads to unclosed energy budgets but justifies the "standard" usage of $-zb$ as a Boussinesq potential energy by the oceanographic community (e.g. sec. 2.4.3 of Vallis, 2017), because $E_{i+p} = c_p\overline{\theta} - z\overline{b} + gz$. However since viscous dissipation is an important quantity for turbulence modelling, we retain this dissipative heating in the temperature budget (45) to work with a properly closed energy budget.

We are now able to specify heat flux, buoyancy flux and mean temperature equation (again neglecting (molecular) diffusive fluxes),

$$\overline{w'\hbar'} = c_p\overline{w'\theta'} - gz(\alpha\overline{w'\theta'} - \beta\overline{w'S'}) = c_p\overline{w'\theta'} - z\overline{w'b'} \tag{46}$$

$$\overline{w'b'} = \alpha\overline{w'\theta'} - \beta\overline{w'S'} \tag{47}$$

$$\partial_t\overline{\theta} + \partial_z\overline{w'\theta'} = \frac{\overline{\epsilon} + \overline{\dot{q}}_{\text{rad}}}{c_p - \alpha g z} \tag{48}$$

Remark that even with very simple thermodynamic modelling such as linearized EOS, the consistent inclusion of salinity as an active tracer lead to non-trivial expression of heat flux.

4 Energy budgets of the SCM

4.1 Consistency of TKE equation with EDMF closures

In this section, we discuss the energetic consistency of a parameterized TKE equation based on the horizontally averaged TKE equation:

$$\partial_t k + \frac{1}{\rho_R}\partial_z(\rho_R T_k) = -\overline{w'\boldsymbol{u}'_h} \cdot \partial_z\overline{\boldsymbol{u}}_h + \overline{w'b'} - \overline{\epsilon} \tag{49}$$

By using energy arguments, we aim to remove ambiguity around three practical topics: how to interpret TKE in the model; whether to use ED or EDMF fluxes in the source terms of TKE; what boundary conditions should be used? Regarding the fluxes, some studies use ED fluxes (Giordani et al., 2020; Hourdin et al., 2019; Han et al., 2016). Other studies use explicitely the full EDMF fluxes (Han & Bretherton, 2019; Witek et al., 2011). However the majority of studies and documentations are ambiguous or not explicit about this point, and modelling choices are often motivated by realism of simulation results based on few test cases. Here, we argue that energy conservation constraints can guide without ambiguity such choices.

If we aim to mimmick the energy budgets of the averaged system (35), then k represents the turbulent kinetic of the whole grid cell, *i.e.* $1/2\overline{\boldsymbol{u}'\cdot\boldsymbol{u}'}$. We keep this choice to stay in line with previous practices. However note that Tan et al. (2018) made a different choice by considering a budget for the *environmental* TKE, $k_e = 1/2\overline{\boldsymbol{u}'_e\cdot\boldsymbol{u}'_e}$.

In (49) sources of TKE arise from the mean kinetic energy via mean shear $-\overline{w'\boldsymbol{u}'_h}\cdot\partial_z\overline{\boldsymbol{u}}_h$, or from internal and potential energies via buoyancy production $\overline{w'b'}$. When the EDMF approach is used to close fluxes in the diagnostic equations of $\overline{\boldsymbol{u}}_h$, $\overline{\theta}$ and $\overline{S}$, then

the same closures must be used in the TKE budget to ensure energetic consistency. As a consequence, the shear term must be closed as

$$-\overline{w'\boldsymbol{u}_h'}\cdot\partial_z\overline{\boldsymbol{u}}_h \underset{\text{EDMF}}{=} -\left[-K_u\partial_z\overline{\boldsymbol{u}}_h + a_p w_p(\boldsymbol{u}_{h,p}-\overline{\boldsymbol{u}}_h)\right]\cdot\partial_z\overline{\boldsymbol{u}}_h \tag{50}$$

In the case of *dry atmosphere*, the buoyancy production term is

$$\overline{w'b'} \underset{\text{EDMF}}{=} \frac{g}{\theta_R}\left[-K_\theta\partial_z\overline{\theta} + a_p w_p(\theta_p-\overline{\theta})\right] \tag{51}$$

whereas in the case of *seawater* with linearized equation of state and $K_b = K_\theta = K_S$,

$$\begin{aligned}\overline{w'b'} &\underset{\text{EDMF}}{=} g\alpha\left[-K_\theta\partial_z\overline{\theta} + a_p w_p(\theta_p-\overline{\theta})\right] - g\beta\left[-K_S\partial_z\overline{S} + a_p w_p(S_p-\overline{S})\right]\\ &= -K_b\partial_z\overline{b} + a_p w_p(b_p-\overline{b})\end{aligned}$$

The flux of TKE T_k is of great importance in convective conditions where non-local transport dominates (Witek et al., 2011). Within the framework exposed in section 2.1, we can apply the two-domain decomposition of the horizontal average to get the exact relation

$$\begin{aligned}\overline{w'\frac{\boldsymbol{u}'\cdot\boldsymbol{u}'}{2}} = \sum_{i=e,p} &\underbrace{a_i\frac{1}{2}\overline{\boldsymbol{u}_i'\cdot\boldsymbol{u}_i'w_i'}}_{\mathrm{I}_i} + \underbrace{a_i(\boldsymbol{u}_i-\overline{\boldsymbol{u}})\cdot\overline{\boldsymbol{u}_i'w_i'}}_{\mathrm{II}_i}\\ &+\underbrace{a_i(w_i-\overline{w})\frac{1}{2}\overline{\boldsymbol{u}_i'\cdot\boldsymbol{u}_i'}}_{\mathrm{III}_i} + \underbrace{a_i\frac{1}{2}\|\boldsymbol{u}_i-\overline{\boldsymbol{u}}\|^2(w_i-\overline{w})}_{\mathrm{IV}_i}\end{aligned} \tag{52}$$

Based on a conditional sampling of plumes on LES, we derive in Part II a simplified EDMF parameterization of T_k encompassing previous approaches existing in the literature, namely

$$\overline{w'\frac{\boldsymbol{u}'\cdot\boldsymbol{u}'}{2}} = \underbrace{-K_k\partial_z k}_{\text{ED}} + \underbrace{\overbrace{a_p w_p(k_p-k)}^{\text{Han \& Bretherton 2019}} + \overbrace{a_p w_p^3}^{\text{Witek et al. 2011}} + \frac{a_p w_p}{2}\|\boldsymbol{u}_{h,p}-\overline{\boldsymbol{u}}_h\|^2}_{\text{new EDMF}} \tag{53}$$

4.2 EDMF-parameterized budgets

Within the anelastic approximation, the budget of resolved kinetic energy, subgrid kinetic energy, and resolved internal+potential energy for a *dry atmosphere* with EDMF closure is

$$\begin{cases}\partial_t E_k + \frac{1}{\rho_R}\partial_z(\rho_R T_{E_k}) &= -K_u(\partial_z\overline{\boldsymbol{u}}_h)^2 + a_p w_p(\boldsymbol{u}_{h,p}-\overline{\boldsymbol{u}}_h)\cdot\partial_z\overline{\boldsymbol{u}}_h\\ \partial_t k + \frac{1}{\rho_R}\partial_z(\rho_R T_k) &= \frac{g}{\theta_R}\left[-K_\theta\partial_z\overline{\theta} + a_p w_p(\theta_p-\overline{\theta})\right] + K_u(\partial_z\overline{\boldsymbol{u}}_h)^2 - a_p w_p(\boldsymbol{u}_{h,p}-\overline{\boldsymbol{u}}_h)\cdot\partial_z\overline{\boldsymbol{u}}_h - \overline{\epsilon}\\ \partial_t E_{i+p} + \frac{1}{\rho_R}\partial_z(\rho_R T_{E_{i+p}}) &= -\frac{g}{\theta_R}\left[-K_\theta\partial_z\overline{\theta} + a_p w_p(\theta_p-\overline{\theta})\right] + \overline{\epsilon} + \overline{\dot{q}}_{\text{rad}}\end{cases} \tag{54}$$

where the flux terms are

$$T_{E_k} = (-K_u\partial_z\overline{\boldsymbol{u}}_h + a_p w_p(\boldsymbol{u}_{h,p}-\overline{\boldsymbol{u}}_h))\cdot\overline{\boldsymbol{u}}_h \tag{55}$$

$$T_{E_{i+p}} = -c_p K_\theta\partial_z\overline{\theta} + c_p a_p w_p(\theta_p-\overline{\theta}) \tag{56}$$

and the associated consistent potential temperature equation is

$$\partial_t\overline{\theta} + \frac{1}{\rho_R}\partial_z\left[\rho_R(-K_\theta\partial_z\overline{\theta} + a_p w_p(\theta_p-\overline{\theta}))\right] = \frac{1}{c_p}\left(\frac{p_R}{p_0}\right)^{-\kappa}(\overline{\epsilon}+\overline{\dot{q}}_{\text{rad}}) \tag{57}$$

Equivalently, in the case of *seawater* with linearized equation of state within the Boussinesq approximation ($\rho_R(z)=\rho_0$),

$$\begin{cases}\partial_t E_k + \partial_z T_{E_k} &= -K_u(\partial_z\overline{\boldsymbol{u}}_h)^2 + a_p w_p(\boldsymbol{u}_{h,p}-\overline{\boldsymbol{u}}_h)\cdot\partial_z\overline{\boldsymbol{u}}_h\\ \partial_t k + \partial_z T_k &= -K_b\partial_z\overline{b} + a_p w_p(b_p-\overline{b}) + K_u(\partial_z\overline{\boldsymbol{u}}_h)^2 - a_p w_p(\boldsymbol{u}_{h,p}-\overline{\boldsymbol{u}}_h)\cdot\partial_z\overline{\boldsymbol{u}}_h - \overline{\epsilon}\\ \partial_t E_{i+p} + \partial_z T_{E_{i+p}} &= -\left(-K_b\partial_z\overline{b} + a_p w_p(b_p-\overline{b})\right) + \overline{\epsilon} + \overline{\dot{q}}_{\text{rad}}\end{cases} \tag{58}$$

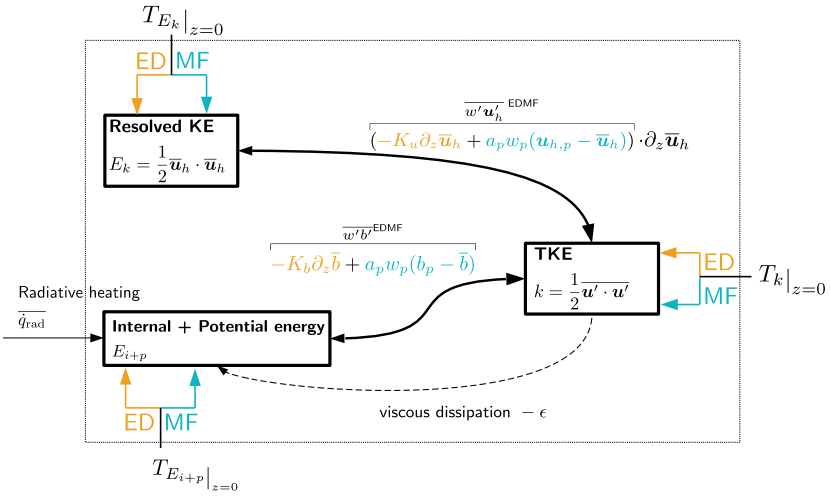

Figure 2: Schematic representation of bulk and boundary energy fluxes within EDMF closure (KE: kinetic energy, TKE: turbulent kinetic energy).

where the flux of internal and potential energy is

$$T_{E_{i+p}} = -\partial_z \left(c_p \left(-K_\theta \partial_z \overline{\theta} + a_p w_p (\theta_p - \overline{\theta}) \right) - z \left(-K_b \partial_z \overline{b} + a_p w_p (b_p - \overline{b}) \right) \right) \quad (59)$$

and the conservative temperature equation is

$$\partial_t \overline{\theta} = \frac{\overline{\epsilon} + \overline{\dot{q}}_{\text{rad}}}{c_p - \alpha g z} - \partial_z \left(-K_\theta \partial_z \overline{\theta} + a_p w_p (\theta_p - \overline{\theta}) \right)$$

A schematic of EDMF energy budgets is provided in Fig. 2.

4.3 Viscous dissipation and eddy-diffusivity

In order to conserve energy we have seen in the previous section that viscous dissipation must be converted into heating. It can be computed in two manners. Either by implementing in the SCM the TKE equation of (54) and using the closure

$$\overline{\epsilon} = \frac{c_\epsilon}{l_\epsilon} k^{3/2}$$

where c_ϵ is a numerical constant and l_ϵ an appropriate length scale. This approach is usually used when eddy-diffusivity is computed as $K_X = c_X l_X \sqrt{k}$ (with c_X a constant and l_X a mixing length). Alternatively dissipation can be computed by assuming a stationary TKE equation and neglecting the transport term, leading to

$$\overline{\epsilon} = \overline{w'b'} - \overline{w'\boldsymbol{u}'_h} \cdot \partial_z \overline{\boldsymbol{u}}_h \quad (60)$$

which is commonly done in SCM using empirical K-profiles (e.g. Han et al., 2016).

4.4 Vertically integrated energy budgets

In this section, we provide global energy budgets to highlight the role of mass-flux terms in bulk energy exchange as well as sinks/sources at boundaries. Let us introduce

the vertical average $\langle X\rangle_z = 1/(\sigma_o^a H)\int_0^{\sigma_o^a H} X\,\mathrm{d}z$, and the boundary operator $[X]_0^{\sigma_o^a H} = 1/(\sigma_o^a H)(X(z=\sigma_o^a H) - X(z=0))$ (with $\sigma_o^a = 1$ in the atmosphere and -1 in the ocean). Then for any advected field X with source term P_X, we have (see Appendix D for a detailed derivation):

$$\begin{aligned}\frac{1}{2}\partial_t\left\langle\rho_R\overline{X}^2\right\rangle_z &= \overbrace{-\left\langle\rho_R K_X(\partial_z\overline{X})^2\right\rangle_z}^{<0} \overbrace{-\left\langle\rho_R\frac{E+D}{2}(X_p-\overline{X})^2\right\rangle_z}^{<0} \\ &\quad+\left\langle\rho_R\overline{X}\,\overline{P}_X\right\rangle_z+\left\langle\rho_R a_p(S_X)_p(X_p-\overline{X})\right\rangle_z \\ &\quad-\left[\rho_R\overline{X}\,\overline{w'X'}+\rho_R a_p w_p\frac{(X_p-\overline{X})^2}{2}\right]_0^{\sigma_o^a H}\end{aligned} \tag{61}$$

Consequently, the entrainment and detrainment processes contribute on average to decreasing the mean variance, similar to eddy-diffusivity terms. Although not sufficient in the context of nonlinear equations, monotonically decreasing variance is usually a necessary property to ensure analytical well-posedness of transport partial differential equations (e.g. Evans, 2010). Interestingly, the last term of the budget implies that a non-zero MF flux at the boundary leads to an additional sink of resolved variance (which is exactly compensated by an equal and opposite boundary source for $\overline{X'^2}$).

We use (61) and the specific source of plume momentum budget (see Appendix D) to get the vertically integrated mean kinetic energy budget,

$$\begin{aligned}\partial_t\left\langle\rho_R E_k\right\rangle_z &= -\left\langle\rho_R K_u(\partial_z\overline{\boldsymbol{u}}_h)^2\right\rangle_z-\left\langle\rho_R\frac{E+D}{2(1-C_u)}\|\boldsymbol{u}_{h,p}-\overline{\boldsymbol{u}}_h\|^2\right\rangle_z \\ &\quad-\left[\rho_R\overline{\boldsymbol{u}}_h\cdot\overline{w'\boldsymbol{u}_h'}\right]_0^{\sigma_o^a H}-\left[\rho_R\frac{a_p w_p}{2(1-C_u)}\|\boldsymbol{u}_{h,p}-\overline{\boldsymbol{u}}_h\|^2\right]_0^{\sigma_o^a H}\end{aligned}$$

Vertically integrating the TKE equation (58) leads to

$$\begin{aligned}\partial_t\left\langle\rho_R k\right\rangle_z &= -\left\langle\rho_R K_b\partial_z\overline{b}\right\rangle_z+\left\langle\rho_R a_p w_p(b_p-\overline{b})\right\rangle_z \\ &\quad+\left\langle\rho_R K_u(\partial_z\overline{\boldsymbol{u}}_h)^2\right\rangle_z+\left\langle\rho_R\frac{E+D}{2(1-C_u)}\|\boldsymbol{u}_{h,p}-\overline{\boldsymbol{u}}_h\|^2\right\rangle_z \\ &\quad-\langle\rho_R\overline{\epsilon}\rangle_z-[\rho_R T_k]_0^{\sigma_o^a H}+\left[\rho_R\frac{a_p w_p}{2(1-C_u)}\|\boldsymbol{u}_{h,p}-\overline{\boldsymbol{u}}_h\|^2\right]_0^{\sigma_o^a H}\end{aligned}$$

where again the MF contribution to shear has been reformulated into a sign-definite bulk production and a boundary term (Appendix D). It allows a clear interpretation: lateral mixing due to either entrainment or detrainment induces a net production of TKE via the shear term, and this production is hyperbolically enhanced if the horizontal drag coefficient C_u is increased. Moreover this provides an energy constraint on C_u, namely $0 \leq C_u < 1$. Additionally, the vertically integrated potential energy and resolved internal energy budget reads

$$\partial_t\left\langle\rho_R E_{i+p}\right\rangle_z = \left\langle\rho_R K_b\partial_z\overline{b}\right\rangle_z-\left\langle\rho_R a_p w_p(b_p-\overline{b})\right\rangle_z+\left\langle\rho_R(\overline{\epsilon}+\overline{q})_{\mathrm{rad}}\right\rangle_z-\left[T_{E_i+\mathcal{E}_p}\right]_0^{\sigma_o^a H} \tag{62}$$

In the three budgets presented above, two different types of source terms appear. The terms in angle bracket $\langle\cdot\rangle_z$ corresponds to bulk conversions of different type of energy and must compensate within each other (excepted for radiative transfer), since no total energy can be created inside the fluid. The terms in square brackets $[\cdot]_0^{\sigma_o^a H}$ are inputs of energy at the boundaries of the fluid which are a net source/sink of total energy (e.g. bottom heating of the atmosphere of surface wind work in the ocean).

4.5 Inconsistent boundary conditions and spurious energy fluxes

In this section, based on the choices made in Pergaud et al. (2009) we provide an example of inconsistent boundary conditions for the plume temperature and the mean temperature resulting in spurious surface heat fluxes in the system.

If we assume that the boundary condition for the mean temperature equation is $-K_\theta \partial_z \overline{\theta}(0) = \overline{w'\theta'}_{\text{sfc}}$ (where $\overline{w'\theta'}_{\text{sfc}}$ is a prescribed surface flux), and that the plume boundary condition is prescribed following Soares et al. (2004)

$$\theta_p(0) = \overline{\theta}(0) + \beta \frac{\overline{w'\theta'}_{\text{sfc}}}{\sqrt{k(0)}} \tag{63}$$

then using (56) the resulting surface flux of E_{i+p} is

$$\begin{aligned} T_{E_{i+p}}(0) &= -c_p K_\theta \partial_z \overline{\theta}(0) + c_p a_p(0) w_p(0)(\theta_p(0) - \overline{\theta}(0)) \\ &= c_p \overline{w'\theta'}_{\text{sfc}} + c_p \overline{w'\theta'}_{\text{sfc}} \frac{a_p(0) w_p(0) \beta}{\sqrt{k(0)}} \end{aligned}$$

where the second term of the r.h.s. is an unphysical source of energy. This bias is due to an inconsistent partioning of the physical boundary flux $c_p \overline{w'\theta'}_{\text{sfc}}$ into ED and MF fluxes. In Pergaud et al. (2009), $w_p(0) = \sqrt{2/3k(0)}$ and $\beta = 0.3$ leading to biases from a few percents up to 25 % depending on the surface value of a_p. In order to correct this bias, on can start from imposing the physical energy flux $T_{Ei+p}(0) = c_p \overline{w'\theta'}_{\text{sfc}}$, then by using its EDMF decomposition (56) and Soares-type plume boundary condition we obtain the consistent Neumann boundary condition for mean temperature

$$\begin{aligned} -K_b(0) \partial_z \overline{\theta}(0) &= \overline{w'\theta'}_{\text{sfc}} - a_p(0) w_p(0)(\theta_p(0) - \overline{\theta}(0)) \\ &= \left(1 - \frac{a_p(0) w_p(0) \beta}{\sqrt{k(0)}}\right) \overline{w'\theta'}_{\text{sfc}} \end{aligned}$$

5 Discussion and conclusion

In this work, we have presented the theoretical derivation of an EDMF scheme with special attention paid to energetic aspects for both dry atmosphere and seawater with linearized equation of state in the anelastic and modernized Boussinesq approximations (Tailleux & Dubos, 2024). Moreover, we provide energy budgets of the scheme, including radiative processes. The derivation systematically reviews approximations used and provides *a priori* scaling estimations. We also documented all necessary subsequent closures necessary to obtain a mass-flux scheme, in order to propose a self-contained introduction to EDMF for oceanographers. Closed energetics at the SCM level is a necessary step to obtain energetically consistent 3D models and thus reduce spurious energy biases. Theoretical horizontally averaged energy budgets are guiding the derivation of consistent energy budgets for SCM with EDMF closure. Besides taking into account MF terms in shear and buoyancy terms, we propose a new MF parameterization of TKE transport. It generalizes previous formulations and implies the consideration of a subplume TKE (Han & Bretherton, 2019). We also show that boundary conditions on both mean and plume variables should be consistent with the EDMF decomposition to avoid spurious energy fluxes at the boundary. Finally we provide a clear interpretation of MF contribution to shear: lateral mixing due to either entrainment or detrainment induces a net production of TKE via the shear term, and such production is enhanced when horizontal drag increases. In a companion paper (Part II, Perrot & Lemarié, 2024), we evaluate EDMF hypotheses in the light of LES of oceanic convection, detail an energy-conserving discretization of the SCM, quantify energy biases of inconsistent formulations.

The development of energetically consistent EDMF schemes can be continued in several ways. First, for real-world applications, the present work has to be extended to more complex thermodynamics models (i.e. moist atmosphere, Pauluis (2008), and seawater with a non-linear equation of state). The proposed framework is flexible enough to be readily extended to other coherent structures of the boundary layer contributing to transport, such as atmospheric downdraft (Han & Bretherton, 2019; Brient et al., 2023).

σ	$= \dfrac{1}{1-a_p}$	Rescaling coefficient
$\overline{w'\phi'}$	$= \sigma a_p w_p(\phi_p - \overline{\phi}) - K_\phi \partial_z \overline{\phi}, \quad \phi = \theta, S$	Vertical turbulent flux for component ϕ
$\overline{w'\boldsymbol{u}'_h}$	$= \sigma a_p w_p(\boldsymbol{u}_{h,p} - \overline{\boldsymbol{u}}_h) - K_m \partial_z \overline{\boldsymbol{u}}_h$	Vertical turbulent momentum flux
$\partial_z(a_p w_p)$	$= E - D$	Plume area conservation equation
$a_p w_p \partial_z \phi_p$	$= \sigma E(\overline{\phi} - \phi_p)$	Plume equation for component ϕ
$a_p w_p \partial_z \boldsymbol{u}_{h,p}$	$= \sigma E(\overline{\boldsymbol{u}}_h - \boldsymbol{u}_{h,p}) + a_p w_p C_u \partial_z \overline{\boldsymbol{u}}_h$	Plume horizontal momentum equation
$a_p w_p \partial_z w_p$	$= -(\sigma b) E w_p + a_p \left\{ a B_p - \sigma_o^a (\sigma b') w_p^2 \right\}$	Plume vertical velocity equation
B_p	$= b_{\text{eos}}(\phi_p) - b_{\text{eos}}(\overline{\phi})$	Buoyancy forcing term
$\partial_t k - \partial_z \left(K_k \partial_z k \right)$	$= K_m (\partial_z \overline{\boldsymbol{u}}_h)^2 - K_b \partial_z \bar{b}$	ED related TKE production terms
	$-\sigma a_p w_p \left((\boldsymbol{u}_{h,p} - \overline{\boldsymbol{u}}_h) \cdot \partial_z \overline{\boldsymbol{u}}_h - (b_p - \bar{b}) \right)$	MF related TKE production terms
	$-\partial_z \left(\sigma a_p w_p \left[k_p - k + \dfrac{1}{2} \lVert \boldsymbol{u}_p - \boldsymbol{u} \rVert^2 \right] \right)$	MF related TKE transport term
	$-\bar{\epsilon}$	TKE dissipation
$a_p w_p \partial_z k_p$	$= \sigma E \left((k - k_p) + (1 + a_p^2 \tilde{\sigma}) \dfrac{1}{2} \lVert \boldsymbol{u}_p - \boldsymbol{u} \rVert^2 \right) -$ $a_p (\epsilon_\nu)_p$	Plume related TKE

Table B1: Same as table 1, but with a relaxation of the small area limit. The small area limit is recovered if $\sigma \equiv 1$ and $\tilde{\sigma} \equiv 0$.

For atmospheric models, the ED-based Monin-Obukhov similarity theory should be reconciled with the EDMF representation of fluxes (Li et al., 2021) to provide unambiguous and consistent boundary conditions and thus avoid potential spurious boundary energy fluxes.

Appendix A Useful identities

$$a_p w_p = -a_e w_e \tag{A1}$$

$$X_p - X_e = \frac{1}{1-a_p}(X_p - \overline{X}) \tag{A2}$$

$$= \frac{1}{-a_p}(X_e - \overline{X}) \tag{A3}$$

$$a_p(w_p - \overline{w})(X_p - \overline{X}) + a_e(w_e - \overline{w})(X_e - \overline{X}) = a_p(1-a_p)(w_p - w_e)(X_p - X_e) \tag{A4}$$

$$= \frac{a_p}{1-a_p}(w_p - \overline{w})(X_p - \overline{X}) \tag{A5}$$

Appendix B Relaxing the small-area assumption

The small-area assumption can be relaxed with no additional complexity if the subplume fluxes $\overline{w'_p X'_p}$ ($X = \theta, S, u, v$) are still neglected. A summary of the EDMF-Energy parameterization in such a regime is presented in Tab. B1.

Appendix C Boundary condition for plume equations

Near the surface, we linearize the plume and mean buoyancy in the form $b_p \simeq b_p^0 + b_p' z$, $\overline{b} \simeq \overline{b}^0 + N_0^2 z$. Then the plume equation for b_p reads at order $O(z^0)$:

$$a_p^0 w_p^0 b_p' = -E_0(b_p^0 - \overline{b}^0)$$

The boundary condition $b_p^0 = \overline{b}^0$ implies that $b_p' = 0$. Thus close to the surface we have

$$b_p(z) \simeq \overline{b}^0, \qquad \overline{b} \simeq \overline{b}^0 + N_0^2 z$$

Then near the surface, the buoyancy force - which is a source of plume momentum and kinetic energy $1/2 w_p^2$ - is at first order $b_p - \overline{b} \simeq -N_0^2 z$. Consequently, any static instability at the surface will result in the absolute growth of the plume vertical momentum ($-N_0^2 z > 0$ in the atmosphere and $-N_0^2 z < 0$ in the ocean).
The boundary condition $b_p(0) = \overline{b}(0)$ implies that at $z = 0$, all the surface flux is allocated in the ED component. Consequently, $N_0^2 = \overline{w'b'}(0)/(-K_b(0)) = \overline{w'b'}(0)/(c_b l_b(0)\sqrt{k(0)})$.
The boundary condition $b_p(0) = \overline{b}(0)$ thus implies that close to the surface

$$b_p(z) \simeq \overline{b}(z) + \frac{\overline{w'b'}(0)}{c_b l_b(0)\sqrt{k_0}} z$$

which has the same form as the Soares-type boundary condition (63).

Appendix D EDMF Mean Variance Equation

Start from the mean and plume equations, and the turbulent flux decomposition

$$\begin{aligned}
\partial_t(\rho_R \overline{X}) &= -\rho_R \partial_z \overline{w'X'} + \rho_R \overline{P}_X && \text{(D1)}\\
\overline{w'X'} &= -K_X \partial_z \overline{X} + a_p w_p (X_p - \overline{X}) && \text{(D2)}\\
a_p w_p \partial_z X_p &= -E(X_p - \overline{X}) + a_p P_{X,p} && \text{(D3)}
\end{aligned}$$

Multiplying the mean equation (D1) by $\overline{X}$ leads to

$$\begin{aligned}
\frac{1}{2}\partial_t \overline{X}^2 &= -\frac{1}{\rho_R}\partial_z(\overline{X}\,\overline{w'X'}) + \overline{w'X'}\partial_z\overline{X} + \overline{X}\,\overline{P_X}\\
&= -\frac{1}{\rho_R}\partial_z(\overline{X}\,\overline{w'X'}) - K_X(\partial_z\overline{X})^2 + a_p w_p (X_p - \overline{X})\partial_z\overline{X} + \overline{X}\,\overline{P_X} && \text{(D4)}
\end{aligned}$$

To rewrite the second term of the right-hand side, we use the plume equation (D2):

$$\begin{aligned}
a_p w_p (X_p - \overline{X})\partial_z \overbrace{\overline{X}}^{=X_p + (\overline{X} - X_p)} &= -E(X_p - \overline{X})^2 + (X_p - \overline{X}) a_p P_{X,p}\\
&\quad -a_p w_p \frac{1}{2}\partial_z (X_p - \overline{X})^2\\
&= -E(X_p - \overline{X})^2 + (X_p - \overline{X}) a_p P_{X,p}\\
&\quad -\frac{1}{\rho_R}\partial_z(\rho_R a_p w_p \frac{1}{2}(X_p - \overline{X})^2)\\
&\quad +(E - D)\frac{1}{2}(X_p - \overline{X})^2\\
&= -(E + D)\frac{1}{2}(X_p - \overline{X})^2 + (X_p - \overline{X}) a_p P_{X,p}\\
&\quad -\frac{1}{\rho_R}\partial_z(\rho_R a_p w_p \frac{1}{2}(X_p - \overline{X})^2)
\end{aligned}$$

Using this expression into equation (D4), then vertically integrating the variance budget leads to the desired equation (61).

We can adapt these computations to deduce the MF contribution to shear production of TKE, knowing that $P_{\boldsymbol{u}_h,p} = C_u w_p \partial_z \overline{\boldsymbol{u}}$. Thus the first equality of the computation is

$$\begin{aligned} a_p w_p(\boldsymbol{u}_{h,p} - \overline{\boldsymbol{u}}_h)\partial_z \overline{\boldsymbol{u}}_h &= -E(\boldsymbol{u}_{h,p} - \overline{\boldsymbol{u}}_h)^2 + C_u a_p w_p(\boldsymbol{u}_{h,p} - \overline{\boldsymbol{u}}_h)\partial_z \overline{\boldsymbol{u}}_h \\ &\quad -a_p w_p \frac{1}{2}\partial_z(\boldsymbol{u}_{h,p} - \overline{\boldsymbol{u}}_h)^2 \\ \implies (1-C_u)a_p w_p(\boldsymbol{u}_{h,p} - \overline{\boldsymbol{u}}_h)\partial_z \overline{\boldsymbol{u}}_h &= -E(\boldsymbol{u}_{h,p} - \overline{\boldsymbol{u}}_h)^2 \\ &\quad -a_p w_p \frac{1}{2}\partial_z(\boldsymbol{u}_{h,p} - \overline{\boldsymbol{u}}_h)^2 \end{aligned}$$

and the rest of the computation follows similarly, justifying the factor $1/(1-C_u)$ in (62).

Appendix E Anelastic energy budgets

In this section, we recall how to derive energy budgets of the anelastic system, following the derivation for compressible fluids of Tailleux (2010) (sec. 2.2), including radiative heating (Weiss, 1994). We then derive temperature equations from the energetically consistent enthalpy budget. Let us start again from the anelastic non-hydrostatic system in advective form coupled to a budget for the specific energy of radiation $\mathcal{E}_r$:

$$\frac{D}{Dt}\boldsymbol{u} = -\nabla\left(\frac{p^\dagger}{\rho_R(z)}\right) + b\boldsymbol{e}_z + \frac{1}{\rho_R}\nabla\cdot(\rho_R\boldsymbol{\tau}) \tag{E1}$$

$$\nabla\cdot(\rho_R(z)\boldsymbol{u}) = 0 \tag{E2}$$

$$\frac{D}{Dt}\eta = \dot{\eta}_{\rm irr} - \frac{1}{\rho_R}\nabla\cdot(\rho_R\boldsymbol{F}_\eta) \tag{E3}$$

$$\frac{D}{Dt}S = -\frac{1}{\rho_R}\nabla\cdot(\rho_R\boldsymbol{F}_S) \tag{E4}$$

$$b = -g\frac{\rho_{\rm EOS} - \rho_R(z)}{\rho_{\rm EOS}} \tag{E5}$$

$$\rho_{\rm EOS} = \rho_{\rm EOS}(\eta, S, p_R(z)) \tag{E6}$$

$$\frac{D}{Dt}\mathcal{E}_r = -\frac{1}{\rho_R}\nabla\cdot(\rho_R\boldsymbol{F}_r) - \dot{q}_{\rm rad} \tag{E7}$$

where $\boldsymbol{\tau}$ is the viscous stress, η is the specific entropy of the fluid (not including entropy of radiation), $\dot{\eta}_{\rm irr}$ is the irreversible production of entropy, $\boldsymbol{F}_\eta$ is the (molecular) diffusive flux of entropy, S is the concentration of an additional component in the fluid (typically salt in the ocean), $\boldsymbol{F}_S$ is the (molecular) diffusive flux of S, $\rho_R(z)$ is a reference density profile, $p_R(z)$ is an associated hydrostatic pressure, i.e. $\mathrm{d}p_R/\mathrm{d}z = -\rho_R g$, $\boldsymbol{F}_r$ is a non-advective radiative flux and $\dot{q}_{\rm rad}$ is an energy transfer term due emission and absorption of radiation, $D/Dt = \partial_t + \boldsymbol{u}\cdot\nabla$ is the Lagrangian derivative.
In contrast with section 2.1 we use specific entropy η instead of potential temperature θ as a state variable. This is motivated by the fact that thermodynamic relationship are written more naturally using η; a consistent equation for θ will be further derived.

The total energy of this system can be advantageously divided into kinetic energy $\rho_R\mathcal{E}_k = \rho_R\frac{1}{2}\boldsymbol{u}\cdot\boldsymbol{u}$, internal energy $\rho_R\mathcal{E}_i = \rho_R(\hbar(\eta,S,p_R(z)) - p_R(z)/\rho_R(z))$ –with $\hbar$ the specific enthalpy–, and potential energy $\rho_R\mathcal{E}_p = \rho_R g z$ (in Tailleux and Dubos (2024) the sum $\mathcal{E}_i + \mathcal{E}_p$ is referred as potential energy), and radiation energy $\rho_R\mathcal{E}_r$. Kinetic energy budget can be derived straightforwardly by taking the scalar product of (E1) with $\rho_R\boldsymbol{u}$, namely

$$\rho_R\frac{D}{Dt}\mathcal{E}_k = -\nabla\cdot(\boldsymbol{u}p^\dagger) + \rho_R w b + \nabla\cdot(\rho_R\boldsymbol{u}\cdot\boldsymbol{\tau}) - \underbrace{\rho_R\boldsymbol{\tau}:\nabla\boldsymbol{u}}_{\rho_R\epsilon} \tag{E8}$$

where ϵ is the viscous dissipation.

E1 Enthalpy budget

Let $F_h(x_\eta, x_S, x_p)$ be the mathematical function defining the enthalpy of a fluid, i.e. if x_η, x_S, x_p are respectively equal to the parcel's entropy, mass of component S and pressure then $F_h(x_\eta, x_S, x_p)$ is the parcel's entropy. Since enthalpy, entropy and mass of component S are extensive variables, we have by definition that for any scalar λ,

$$F_h(\lambda x_\eta, \lambda x_S, x_p) = \lambda F_h(x_\eta, x_S, x_p) \tag{E9}$$

which in turn implies that by virtue of Euler's homogeneous function theorem,

$$F_h(x_\eta, x_S, x_p) = x_\eta \frac{\partial F_h}{x_\eta} + x_S \frac{\partial F_h}{\partial x_S} \tag{E10}$$

Now let η^V and S^V be respectively entropy and mass of component S *per unit volume* of the fluid, i.e. $h^V = \rho_R(z)\hbar$, $\eta^V = \rho_R(z)\eta$, $S^V = \rho_R(z)S$. Previous properties on F_h allow to define the enthalpy per unit volume,

$$\hbar^V = F_h(\eta^V, S^V, p) = \rho_R \hbar = \eta^V \frac{\partial F_h}{x_\eta}(\eta^V, S^V, p) + S^V \frac{\partial F_h}{\partial x_S}(\eta^V, S^V, p) \tag{E11}$$

Finally, equating the gradient of $\hbar^V = F_h(\eta^V, S^V, p)$ and of $\hbar^V = \eta^V \frac{\partial F_h}{x_\eta}(\eta^V, S^V, p) + S^V \frac{\partial F_h}{\partial x_S}(\eta^V, S^V, p)$, we derive the useful relation:

$$\frac{\partial F_h}{x_p}(\eta^V, S^V, p)\nabla p = \eta^V \nabla \frac{\partial F_h}{x_\eta}(\eta^V, S^V, p) + S^V \nabla \frac{\partial F_h}{\partial x_S}(\eta^V, S^V, p) \tag{E12}$$

Now, on can compute the evolution of $\hbar^V$,

$$\begin{aligned}
\partial_t \hbar^V + \nabla \cdot (\hbar^V \boldsymbol{u}) &= \frac{\partial F_h}{\partial x_\eta}\partial_t \eta^V + \frac{\partial F_h}{\partial x_S}\partial_t S^V + \frac{\partial F_h}{\partial x_p}\partial_t p \\
&\quad + \nabla \cdot ((\eta^V \frac{\partial F_h}{x_\eta} + S^V \frac{\partial F_h}{\partial x_S})\boldsymbol{u}) \\
&= \frac{\partial F_h}{\partial x_\eta}(\partial_t \eta^V + \nabla \cdot (\eta^V \boldsymbol{u})) \\
&\quad + \frac{\partial F_h}{\partial x_S}(\partial_t S^V + \nabla \cdot (S^V \boldsymbol{u})) \\
&\quad + \frac{\partial F_h}{\partial x_p}(\partial_t p + \boldsymbol{u} \cdot \nabla p) \\
&\quad + \underbrace{\eta^V \boldsymbol{u} \cdot (\frac{\partial F_h}{\partial x_\eta}) + S^V \boldsymbol{u} \cdot (\frac{\partial F_h}{\partial x_S}) - \frac{\partial F_h}{\partial x_p}\boldsymbol{u} \cdot \nabla p}_{=0,\text{(E12)}}
\end{aligned}$$

Now using $\mathrm{d}\hbar^V = \rho_R V \mathrm{d}p + T\mathrm{d}\eta^V + \mu \mathrm{d}S^V$ (where μ is the chemical potential of S) and $V = 1/\rho_{\mathrm{EOS}}$, we obtain $\frac{\partial F_h}{\partial x_\eta}(\eta^V, S^V, p) = T$, $\frac{\partial F_h}{\partial x_p}(\eta^V, S^V, p) = \rho_R/\rho_{\mathrm{EOS}} = 1 + b/g$, $\frac{\partial F_h}{\partial x_S}(\eta^V, S^V, p)$. Evaluating the enthalpy equation at $p = p_R$, using η and S budgets and integrating by part leads to

$$\begin{aligned}
\partial_t(\rho_R \hbar) + \nabla \cdot (\rho_R \hbar \boldsymbol{u}) &= (1 + b/g)(-\rho_R g w) \\
&\quad + \rho_R \left(T\dot{\eta}_{\mathrm{irr}} + \boldsymbol{F}_\eta \cdot \nabla T + \boldsymbol{F}_S \cdot \nabla \mu\right) \\
&\quad - \nabla \cdot \left(\rho_R \left[T\boldsymbol{F}_\eta + \mu \boldsymbol{F}_S\right]\right)
\end{aligned} \tag{E13}$$

where the first source on the right-hand side corresponds to the work of pressure forces, the second one is a production of enthalpy due to irreversible production of entropy and diffusion of entropy and S, and the last term is the divergence of a diffusive flux of enthalpy. In the remainder of this section, we will denote it $\boldsymbol{F}_\hbar = T\boldsymbol{F}_\eta + \mu \boldsymbol{F}_S$.

E2 Total energy conservation and entropy production

Using relation $\mathcal{E}_i = \hbar - p_R/\rho_R$, we can combine the previous expression to obtain the total energy budget in advective form

$$\rho_R \frac{D}{Dt}(\mathcal{E}_k + \mathcal{E}_i + \mathcal{E}_p + \mathcal{E}_r) = \nabla \cdot (\rho_R \boldsymbol{F}_{\rm tot}) + \rho_R \dot{\mathcal{E}}_{\rm tot} \tag{E14}$$

where the non-advective flux of total energy and the net production of total energy are

$$\rho_R \boldsymbol{F}_{\rm tot} = -\boldsymbol{u}(p^\dagger + p_R) + \rho_R \left[\boldsymbol{u}\cdot\boldsymbol{\tau} - T\boldsymbol{F}_\eta - \mu \boldsymbol{F}_S - \boldsymbol{F}_r\right] \tag{E15}$$

$$\rho_R \dot{\mathcal{E}}_{\rm tot} = \rho_R \left(T\dot{\eta}_{\rm irr} + \boldsymbol{F}_\eta \cdot \nabla T + \boldsymbol{F}_S \cdot \nabla \mu - \epsilon - \dot{q}_{\rm rad}\right) \tag{E16}$$

Thus total energy is conserved if and only if $\dot{\mathcal{E}}_{\rm tot}$ vanishes, leading to the constraint

$$\dot{\eta}_{\rm irr} = \underbrace{\frac{\epsilon - \boldsymbol{F}_\eta \cdot \nabla T - \boldsymbol{F}_S \cdot \nabla \mu}{T}}_{\text{material prod.}} + \underbrace{\frac{\dot{q}_{\rm rad}}{T}}_{\text{radiative prod.}} \tag{E17}$$

In order to illustrate the energy conversion between the different energy reservoirs, one can write

$$\begin{cases} \rho_R \frac{D}{Dt}\mathcal{E}_k = \nabla \cdot (-\boldsymbol{u}p^\dagger + \rho_R \boldsymbol{u}\cdot\boldsymbol{\tau}) + \rho_R w b - \rho_R \epsilon \\ \rho_R \frac{D}{Dt}\mathcal{E}_i = \nabla \cdot (-\boldsymbol{u}p_R + \rho_R \left[-T\boldsymbol{F}_\eta - \mu \boldsymbol{F}_S\right]) - \rho_R g w - \rho_R w b + \rho_R \epsilon + \rho_R \dot{q}_{\rm rad} \\ \rho_R \frac{D}{Dt}\mathcal{E}_p = \rho_R g w \\ \rho_R \frac{D}{Dt}\mathcal{E}_r = -\nabla \cdot (\rho_R \boldsymbol{F}_r) - \rho_R \dot{q}_{\rm rad} \end{cases} \tag{E18}$$

E3 Temperature equation

The constraint on entropy production derived above ensures that the enthalpy budget (E13) is energetically consistent. It is more convenient to work with temperature than enthalpy, since enthalpy is not observable. In this section, we will derive temperature equations from enthalpy budgets, which ensures that temperature budgets remain energetically consistent.

E31 Anelastic dry air

For dry air in the anelastic approximation, specific enthalpy and buoyancy reads

$$\hbar(\theta, p_R(z)) = c_p T = c_p \theta \left(\frac{p_R(z)}{p_0}\right)^\kappa \tag{E19}$$

$$b = -\partial_z(\hbar + gz) = g\frac{\theta - \theta_R(z)}{\theta_R(z)} \tag{E20}$$

where c_p is a constant specific heat capacity of dry air, p_0 is a constant pressure reference, θ is the potential temperature, $\theta_R(z) = p_R \left(\frac{p_R(z)}{p_0}\right)^{-\kappa}/(\rho_R R_d)$ is the reference potential temperature profile, R_d is the specific dry air ideal constant, $\kappa = R_d/c_p$. We straightforwardly obtain an equation for potential temperature using the enthalpy budget (E13):

$$c_p \left(\frac{p_R}{p_0}\right)^\kappa \partial_t \theta + \frac{1}{\rho_R}\nabla \cdot \left(\rho_R c_p \left(\frac{p_R}{p_0}\right)^\kappa \theta \boldsymbol{u} + \rho_R \boldsymbol{F}_\hbar\right) = -gw - g\frac{\theta - \theta_R(z)}{\theta_R(z)} w + \epsilon + \dot{q}_{\rm rad} \tag{E21}$$

which can be rewritten after some algebra as

$$\partial_t \theta + \frac{1}{\rho_R}\nabla \cdot (\rho_R \theta \boldsymbol{u}) + \frac{1}{c_p}\left(\frac{p_R}{p_0}\right)^{-\kappa} \nabla \cdot (\rho_R \boldsymbol{F}_\hbar) = \frac{1}{c_p}\left(\frac{p_R}{p_0}\right)^{-\kappa} (\epsilon + \dot{q}_{\rm rad}) \tag{E22}$$

The elimination of the buoyancy flux $-wb$ on the r.h.s of the budget unveils the advantage of working with potential temperature instead of in situ temperature.

E32 Boussinesq seawater with a linearized EOS

For seawater with a linearized EOS in Boussinesq approximation ($\rho_R(z) = \rho_0$) buoyancy reads

$$b = -\partial_z(\hbar + gz) = g\alpha(\theta - \theta_0) - \beta(S - S_0) \tag{E23}$$

and the corresponding enthalpy can be formed as

$$\hbar(\theta, S, p_R(z)) = c_p\theta + \overbrace{\frac{p_R(z) - p_0}{\rho_0}}^{-gz}(1 + \alpha(\theta - \theta_0) - \beta(S - S_0)) \tag{E24}$$

where c_p is a constant specific heat capacity of seawater, p_0 and ρ_0 are constant pressure and density references, α is the thermal expansion coefficient and β is the haline contraction coefficient. For a linearized equation of state potential and conservative temperature coincide, and they are denoted by θ. They are related to in-situ temperature T by the formula

$$T = \left(1 + \alpha\frac{p_R - p_0}{\rho_0 c_p}\right)\theta \tag{E25}$$

Inserting the enthalpy expression (E24) into the enthalpy budget (E13) leads to

$$c_p\frac{D}{Dt}\theta + \frac{D}{Dt}(-zg) + \frac{D}{Dt}(-zb) = -wg - wb + \epsilon + \dot{q}_{\text{rad}} - \nabla\cdot\boldsymbol{F}_\hbar \tag{E26}$$

$$\implies c_p\frac{D}{Dt}\theta - z\frac{D}{Dt}b = \epsilon + \dot{q}_{\text{rad}} - \nabla\cdot\boldsymbol{F}_\hbar \tag{E27}$$

Since $\frac{D}{Dt}S = -\nabla\cdot\boldsymbol{F}_S$, we have $\frac{D}{Dt}b = g\alpha\frac{D}{Dt}\theta + g\beta\nabla\cdot\boldsymbol{F}_S$. Thus using (E27) we obtain the energetically consistent conservative temperature equation

$$\frac{D}{Dt}\theta = \frac{\epsilon + \dot{q}_{\text{rad}} - \nabla\cdot\boldsymbol{F}_\hbar + zg\beta\nabla\cdot\boldsymbol{F}_S}{c_p - \alpha gz} \tag{E28}$$

Again the elimination of the buoyancy flux in the r.h.s of the budget unveils the advantage of using conservative temperature. It can be use to compute the budget of the "pseudo"-potential energy $-zb$,

$$\frac{D}{Dt}(-zb) = -wb - z\alpha g\frac{\epsilon + \dot{q}_{\text{rad}} - \nabla\cdot\boldsymbol{F}_\hbar + zg\beta\nabla\cdot\boldsymbol{F}_S}{c_p - \alpha gz} + z\beta g\nabla\cdot\boldsymbol{F}_S \tag{E29}$$

Let us remark that the sum of potential and internal energy is $\mathcal{E}_i + \mathcal{E}_p = \hbar - p_R/\rho_R + gz = c_p\theta - zb + gz$. Neglecting molecular diffusion, viscous dissipation and radiative heating, this splitting justifies the common use of $-zb$ as a proxy for "potential" energy in oceanography (e.g. Olbers et al., 2012). We nevertheless retain these terms in the temperature budget (E28) to work with a properly closed energy budget.

Open Research

Figures were created with Mathcha (www.mathcha.io/). No data were used for this study.

Acknowledgments

The authors would like to thank Hilary Weller and two anonymous reviewers for their constructive comments to help improve our manuscript. This work was supported by the *institut des Mathématiques pour la Planète Terre* (iMPT) through the project "Coherent sub-grid scale modeling for ocean climate models". It was carried out as part of the technological defense project PROTEVS2 under the auspices of the French Ministry of the Armies / DGA. MP was supported by a PhD fellowship from Ecole Normale Supérieure Paris. This research was partially funded by l'Agence Nationale de la Recherche (ANR), project ANR-23-CE01-0009.

References

Arakawa, A., & Schubert, W. H. (1974). Interaction of a Cumulus Cloud Ensemble with the Large-Scale Environment, Part I. *J. Atmos. Sci.*, *31*(3), 674–701. doi: 10.1175/1520-0469(1974)031⟨0674:IOACCE⟩2.0.CO;2

Bony, S., Stevens, B., Frierson, D. M. W., Jakob, C., Kageyama, M., Pincus, R., ... Webb, M. J. (2015). Clouds, circulation and climate sensitivity. *Nat. Geosci.*, *8*(4), 261–268. doi: 10.1038/ngeo2398

Bretherton, C. S., McCaa, J. R., & Grenier, H. (2004, April). A New Parameterization for Shallow Cumulus Convection and Its Application to Marine Subtropical Cloud-Topped Boundary Layers. Part I: Description and 1D Results. *Monthly Weather Review*, *132*(4), 864–882. Retrieved from `https://journals.ametsoc.org/view/journals/mwre/132/4/1520-0493_2004_132_0864_anpfsc_2.0.co_2.xml` doi: 10.1175/1520-0493(2004)132⟨0864:ANPFSC⟩2.0.CO;2

Brient, F., Couvreux, F., Rio, C., & Honnert, R. (2023). Coherent subsiding structures in large eddy simulations of atmospheric boundary layers. *Quart. J. Roy. Meteorol. Soc.*. doi: 10.1002/qj.4625

Burchard, H. (2002). Energy-conserving discretisation of turbulent shear and buoyancy production. *Ocean Modell.*, *4*(3-4), 347–361. doi: 10.1016/S1463-5003(02)00009-4

Cohen, Y., Lopez-Gomez, I., Jaruga, A., He, J., Kaul, C. M., & Schneider, T. (2020, September). Unified Entrainment and Detrainment Closures for Extended Eddy-Diffusivity Mass-Flux Schemes. *Journal of Advances in Modeling Earth Systems*, *12*(9). Retrieved 2021-11-02, from `https://onlinelibrary.wiley.com/doi/10.1029/2020MS002162` doi: 10.1029/2020MS002162

Couvreux, F., Guichard, F., Masson, V., & Redelsperger, J.-L. (2007). Negative water vapour skewness and dry tongues in the convective boundary layer: observations and large-eddy simulation budget analysis. *Bound.-Lay. Meteorol.*, *123*(2), 269–294. doi: 10.1007/s10546-006-9140-y

Deardorff, J. W. (1966). The Counter-Gradient Heat Flux in the Lower Atmosphere and in the Laboratory. *J. Atmos. Sci.*, *23*(5), 503–506. doi: 10.1175/1520-0469(1966)023⟨0503:TCGHFI⟩2.0.CO;2

Deardorff, J. W. (1970). Convective Velocity and Temperature Scales for the Unstable Planetary Boundary Layer and for Rayleigh Convection. *J. Atmos. Sci.*, *27*(8), 1211–1213. doi: 10.1175/1520-0469(1970)027⟨1211:CVATSF⟩2.0.CO;2

Denbo, D. W., & Skyllingstad, E. D. (1996). An ocean large-eddy simulation model with application to deep convection in the Greenland Sea. *J. Geophys. Res.*, *101*(C1), 1095–1110. doi: 10.1029/95JC02828

de Rooy, W. C., Bechtold, P., Fröhlich, K., Hohenegger, C., Jonker, H., Mironov, D., ... Yano, J.-I. (2013). Entrainment and detrainment in cumulus convection: an overview. *Quart. J. Roy. Meteorol. Soc.*, *139*(670), 1–19. doi: 10.1002/qj.1959

Eden, C. (2016). Closing the energy cycle in an ocean model. *Ocean Modell.*, *101*, 30–42. doi: 10.1016/j.ocemod.2016.02.005

Eden, C., & Olbers, D. (2014). An Energy Compartment Model for Propagation, Nonlinear Interaction, and Dissipation of Internal Gravity Waves. *J. Phys. Oceanogr.*, *44*(8), 2093–2106. doi: 10.1175/JPO-D-13-0224.1

Eldred, C., & Gay-Balmaz, F. (2021). Thermodynamically consistent semi-compressible fluids: a variational perspective. *J. Phys. A Math. Theor.*, *54*, 345701. doi: 10.1088/1751-8121/ac1384

Evans, L. C. (2010). *Partial Differential Equations*. American Mathematical Soc.

Fox-Kemper, B., Adcroft, A., Böning, C. W., Chassignet, E. P., Curchitser, E., Danabasoglu, G., ... Yeager, S. G. (2019). Challenges and Prospects in Ocean Circulation Models. *Front. Mar. Sci.*, *6*, 65. doi: 10.3389/fmars.2019.00065

Garanaik, A., Pereira, F. S., Smith, K., Robey, R., Li, Q., Pearson, B., & Van Roekel, L. (2024). A New Hybrid Mass-Flux/High-Order Turbulence Closure for Ocean Vertical Mixing. *Journal of Advances in Modeling Earth Systems*, *16*(1). Retrieved 2024-01-31, from `https://onlinelibrary.wiley.com/doi/abs/10.1029/2023MS003846` (_eprint: https://onlinelibrary.wiley.com/doi/pdf/10.1029/2023MS003846) doi: 10.1029/2023MS003846

Garratt, J. (1994). Review: the atmospheric boundary layer. *Earth-Science Reviews*, *37*(1-2), 89–134. doi: 10.1016/0012-8252(94)90026-4

Giordani, H., Bourdallé-Badie, R., & Madec, G. (2020). An Eddy-Diffusivity Mass-Flux Parameterization for Modeling Oceanic Convection. *J. Adv. Model. Earth Syst.*, *12*. doi: 10.1029/2020MS002078

Gregory, D., Kershaw, R., & Inness, P. M. (1997). Parametrization of momentum transport by convection. II: Tests in single-column and general circulation models. *Quart. J. Roy. Meteorol. Soc.*, *123*(541), 1153–1183. doi: 10.1002/qj.49712354103

Hahn, D. W., & Özişik, M. N. (2012). *Heat Conduction* (1st ed.). Wiley. doi: 10.1002/9781118411285

Han, J., & Bretherton, C. S. (2019). TKE-Based Moist Eddy-Diffusivity Mass-Flux (EDMF) Parameterization for Vertical Turbulent Mixing. *Weather Forecast.*, *34*(4), 869–886. doi: 10.1175/WAF-D-18-0146.1

Han, J., Witek, M. L., Teixeira, J., Sun, R., Pan, H.-L., Fletcher, J. K., & Bretherton, C. S. (2016, February). Implementation in the NCEP GFS of a Hybrid Eddy-Diffusivity Mass-Flux (EDMF) Boundary Layer Parameterization with Dissipative Heating and Modified Stable Boundary Layer Mixing. *Weather and Forecasting*, *31*(1), 341–352. Retrieved 2024-06-17, from `https://journals.ametsoc.org/view/journals/wefo/31/1/waf-d-15-0053_1.xml` (Publisher: American Meteorological Society Section: Weather and Forecasting) doi: 10.1175/WAF-D-15-0053.1

He, J., Cohen, Y., Lopez-Gomez, I., Jaruga, A., & Schneider, T. (2021, May). *An Improved Perturbation Pressure Closure for Eddy-Diffusivity Mass-Flux Schemes* [preprint]. Retrieved 2021-11-02, from `http://www.essoar.org/doi/10.1002/essoar.10505084.2` (Archive Location: world Publisher: Earth and Space Science Open Archive Section: Atmospheric Sciences) doi: 10.1002/essoar.10505084.2

Higgins, C. W., Katul, G. G., Froidevaux, M., Simeonov, V., & Parlange, M. B. (2013). Are atmospheric surface layer flows ergodic? *Geophys. Res. Lett.*, *40*(12), 3342–3346.

Holtslag, A. A. M., & Moeng, C.-H. (1991). Eddy diffusivity and countergradient transport in the convective atmospheric boundary layer. *J. Atmos. Sci.*, *48*(14), 1690 - 1698. doi: https://doi.org/10.1175/1520-0469(1991)048⟨1690:EDACTI⟩2.0.CO;2

Honnert, R., Couvreux, F., Masson, V., & Lancz, D. (2016). Sampling the Structure of Convective Turbulence and Implications for Grey-Zone Parametrizations. *Bound.-Lay. Meteorol.*, *160*(1), 133–156. doi: 10.1007/s10546-016-0130-4

Hourdin, F., Couvreux, F., & Menut, L. (2002). Parameterization of the Dry Convective Boundary Layer Based on a Mass Flux Representation of Thermals. *J. Atmos. Sci.*, *59*(6), 1105–1123. doi: 10.1175/1520-0469(2002)059⟨1105:POTDCB⟩2.0.CO;2

Hourdin, F., Jam, A., Rio, C., Couvreux, F., Sandu, I., Lefebvre, M.-P., ... Idelkadi, A. (2019). Unified parameterization of convective boundary layer transport and clouds with the thermal plume model. *Journal of Advances in Modeling Earth Systems*, *11*(9), 2910–2933. Retrieved 2024-01-09, from `https://onlinelibrary.wiley.com/doi/abs/10.1029/2019MS001666` (_eprint: https://onlinelibrary.wiley.com/doi/pdf/10.1029/2019MS001666)

doi: 10.1029/2019MS001666

Jansen, M. F., Adcroft, A., Khani, S., & Kong, H. (2019). Toward an Energetically Consistent, Resolution Aware Parameterization of Ocean Mesoscale Eddies. *J. Adv. Model. Earth Syst.*, *11*(8), 2844–2860. doi: 10.1029/2019MS001750

Johansson, C., Smedman, A.-S., Högström, U., Brasseur, J. G., & Khanna, S. (2001). Critical Test of the Validity of Monin–Obukhov Similarity during Convective Conditions. *J. Atmos. Sci.*, *58*(12), 1549–1566. doi: 10.1175/1520-0469(2001)058⟨1549:CTOTVO⟩2.0.CO;2

Kato, H., & Phillips, O. M. (1969). On the penetration of a turbulent layer into stratified fluid. *J. Fluid Mech.*, *37*(4), 643–655. doi: 10.1017/S0022112069000784

Kuo, Y., & Neelin, J. D. (2022, October). Conditions for Convective Deep Inflow. *Geophysical Research Letters*, *49*(20), e2022GL100552. Retrieved 2024-07-02, from `https://agupubs.onlinelibrary.wiley.com/doi/10.1029/2022GL100552` doi: 10.1029/2022GL100552

Large, W. G., McWilliams, J. C., & Doney, S. C. (1994). Oceanic vertical mixing: A review and a model with a nonlocal boundary layer parameterization. *Rev. Geophys.*, *32*(4), 363–403. doi: 10.1029/94RG01872

Lauritzen, P. H., Kevlahan, N. K.-R., Toniazzo, T., Eldred, C., Dubos, T., Gassmann, A., ... Bacmeister, J. T. (2022). Reconciling and Improving Formulations for Thermodynamics and Conservation Principles in Earth System Models (ESMs). *J. Adv. Model. Earth Syst.*, *14*(9), e2022MS003117. doi: 10.1029/2022MS003117

LeVeque, R. J. (2002). *Finite volume methods for hyperbolic problems* (Vol. 31). Cambridge university press.

Li, Q., Cheng, Y., & Gentine, P. (2021). Connection Between Mass Flux Transport and Eddy Diffusivity in Convective Atmospheric Boundary Layers. *Geophys. Res. Lett.*, *48*(8), e2020GL092073. doi: 10.1029/2020GL092073

Li, Q., Gentine, P., Mellado, J. P., & McColl, K. A. (2018). Implications of Nonlocal Transport and Conditionally Averaged Statistics on Monin–Obukhov Similarity Theory and Townsend's Attached Eddy Hypothesis. *J. Atmos. Sci.*, *75*(10), 3403–3431. doi: 10.1175/JAS-D-17-0301.1

Madec, G., Bourdallé-Badie, R., Chanut, J., Clementi, E., Coward, A., Ethé, C., ... Samson, G. (2019). *NEMO ocean engine.* Retrieved from `https://zenodo.org/record/1464816` doi: 10.5281/ZENODO.1464816

Madec, G., Delecluse, P., Crepon, M., & Chartier, M. (1991). A Three-Dimensional Numerical Study of Deep-Water Formation in the Northwestern Mediterranean Sea. *J. Phys. Oceanogr.*, *21*(9), 1349–1371. doi: 10.1175/1520-0485(1991)021⟨1349:ATDNSO⟩2.0.CO;2

Marshall, J., Hill, C., Perelman, L., & Adcroft, A. (1997). Hydrostatic, quasi-hydrostatic, and nonhydrostatic ocean modeling. *J. Geophys. Res.*, *102*(C3), 5733–5752. doi: 10.1029/96JC02776

Martin, T., Park, W., & Latif, M. (2013). Multi-centennial variability controlled by Southern Ocean convection in the Kiel Climate Model. *Clim. Dynam.*, *40*(7), 2005–2022. doi: 10.1007/s00382-012-1586-7

McDougall, T. J. (2003). Potential Enthalpy: A Conservative Oceanic Variable for Evaluating Heat Content and Heat Fluxes. *J. Phys. Oceanogr.*, *33*(5), 945–963. doi: 10.1175/1520-0485(2003)033⟨0945:PEACOV⟩2.0.CO;2

Moore, G. W. K., Våge, K., Pickart, R. S., & Renfrew, I. A. (2015). Decreasing intensity of open-ocean convection in the Greenland and Iceland seas. *Nat. Clim. Change*, *5*(9), 877–882. doi: 10.1038/nclimate2688

Olbers, D., Willebrand, J., & Eden, C. (2012). *Ocean Dynamics.* Berlin, Heidelberg: Springer Berlin Heidelberg. doi: 10.1007/978-3-642-23450-7

Pauluis, O. (2008). Thermodynamic Consistency of the Anelastic Approximation for a Moist Atmosphere. *J. Atmos. Sci.*, *65*, 2719–2729. doi:

10.1175/2007JAS2475.1

Pergaud, J., Masson, V., Malardel, S., & Couvreux, F. (2009). A Parameterization of Dry Thermals and Shallow Cumuli for Mesoscale Numerical Weather Prediction. *Bound.-Lay. Meteorol.*, *132*, 83–106. doi: 10.1007/s10546-009-9388-0

Perrot, M., & Lemarié, F. (2024, August). *Energetically consistent eddy-diffusivity mass-flux convective schemes. part ii: Implementation and evaluation in an oceanic context.*

Peters, J. M. (2016, November). The Impact of Effective Buoyancy and Dynamic Pressure Forcing on Vertical Velocities within Two-Dimensional Updrafts. *Journal of the Atmospheric Sciences*, *73*(11), 4531–4551. Retrieved 2024-07-02, from `https://journals.ametsoc.org/view/journals/atsc/73/11/jas-d-16-0016.1.xml` (Publisher: American Meteorological Society Section: Journal of the Atmospheric Sciences) doi: 10.1175/JAS-D-16-0016.1

Peters, J. M., Morrison, H., Zhang, G. J., & Powell, S. W. (2021). Improving the Physical Basis for Updraft Dynamics in Deep Convection Parameterizations. *Journal of Advances in Modeling Earth Systems*, *13*(2), e2020MS002282. Retrieved 2024-07-02, from `https://onlinelibrary.wiley.com/doi/abs/10.1029/2020MS002282` (_eprint: https://onlinelibrary.wiley.com/doi/pdf/10.1029/2020MS002282) doi: 10.1029/2020MS002282

Piron, A., Thierry, V., Mercier, H., & Caniaux, G. (2016). Argo float observations of basin-scale deep convection in the Irminger sea during winter 2011–2012. *Deep-Sea Res. I*, *109*, 76–90. doi: 10.1016/j.dsr.2015.12.012

Ramadhan, A., Wagner, G. L., Hill, C., Campin, J.-M., Churavy, V., Besard, T., ... Marshall, J. (2020). Oceananigans.jl: Fast and friendly geophysical fluid dynamics on GPUs. *Journal of Open Source Software*, *5*(53), 2018. Retrieved from `https://doi.org/10.21105/joss.02018` doi: 10.21105/joss.02018

Resseguier, V., Mémin, E., & Chapron, B. (2017). Geophysical flows under location uncertainty, Part II Quasi-geostrophy and efficient ensemble spreading. *Geophys. Astrophys. Fluid Dyn.*, *111*(3), 177–208.

Rio, C., Hourdin, F., Couvreux, F., & Jam, A. (2010). Resolved Versus Parametrized Boundary-Layer Plumes. Part II: Continuous Formulations of Mixing Rates for Mass-Flux Schemes. *Bound.-Lay. Meteorol.*, *135*(3), 469–483. doi: 10.1007/s10546-010-9478-z

Romps, D. M., & Charn, A. B. (2015). Sticky thermals: Evidence for a dominant balance between buoyancy and drag in cloud updrafts. *Journal of the Atmospheric Sciences*, *72*(8), 2890 - 2901. Retrieved from `https://journals.ametsoc.org/view/journals/atsc/72/8/jas-d-15-0042.1.xml` doi: 10.1175/JAS-D-15-0042.1

Roode, S. R. d., Siebesma, A. P., Jonker, H. J. J., & Voogd, Y. d. (2012). Parameterization of the Vertical Velocity Equation for Shallow Cumulus Clouds. *Mon. Weather Rev.*, *140*(8), 2424–2436. doi: 10.1175/MWR-D-11-00277.1

Rotunno, R., & Klemp, J. B. (1982). The Influence of the Shear-Induced Pressure Gradient on Thunderstorm Motion. *Mon. Weather Rev.*, *110*(2), 136–151. doi: 10.1175/1520-0493(1982)110⟨0136:TIOTSI⟩2.0.CO;2

Schmidt, H., & Schumann, U. (1989). Coherent structure of the convective boundary layer derived from large-eddy simulations. *J. Fluid Mech.*, *200*, 511–562. doi: 10.1017/S0022112089000753

Schmitt, F. G. (2007). About Boussinesq's turbulent viscosity hypothesis: historical remarks and a direct evaluation of its validity. *Comptes Rendus Mécanique*, *335*(9), 617–627. doi: 10.1016/j.crme.2007.08.004

Schneider, T., Teixeira, J., Bretherton, C. S., Brient, F., Pressel, K. G., Schär, C., & Siebesma, A. P. (2017). Climate goals and computing the future of clouds. *Nat. Clim. Change*, *7*(1), 3–5. doi: 10.1038/nclimate3190

Siebesma, A. P., Soares, P. M. M., & Teixeira, J. (2007). A Combined Eddy-

Diffusivity Mass-Flux Approach for the Convective Boundary Layer. *J. Atmos. Sci.*, *64*(4), 1230–1248. doi: 10.1175/JAS3888.1

Simpson, J., & Wiggert, V. (1969). Models of precipitating cumulus towers. *Monthly Weather Review*, *97*(7), 471 - 489. Retrieved from https://journals.ametsoc.org/view/journals/mwre/97/7/1520-0493_1969_097_0471_mopct_2_3_co_2.xml doi: 10.1175/1520-0493(1969)097⟨0471:MOPCT⟩2.3.CO;2

Soares, P. M. M., Miranda, P. M. A., Siebesma, A. P., & Teixeira, J. (2004). An eddy-diffusivity/mass-flux parametrization for dry and shallow cumulus convection. *Quart. J. Roy. Meteorol. Soc.*, *130*(604), 3365–3383. doi: 10.1256/qj.03.223

Tailleux, R. (2010). Identifying and quantifying nonconservative energy production/destruction terms in hydrostatic Boussinesq primitive equation models. *Ocean Modell.*, *34*(3), 125–136. doi: 10.1016/j.ocemod.2010.05.003

Tailleux, R., & Dubos, T. (2024, April). A simple and transparent method for improving the energetics and thermodynamics of seawater approximations: Static energy asymptotics (SEA). *Ocean Modelling*, *188*, 102339. Retrieved 2024-05-07, from https://www.sciencedirect.com/science/article/pii/S146350032400026X doi: 10.1016/j.ocemod.2024.102339

Tan, Z., Kaul, C. M., Pressel, K. G., Cohen, Y., Schneider, T., & Teixeira, J. (2018). An Extended Eddy-Diffusivity Mass-Flux Scheme for Unified Representation of Subgrid-Scale Turbulence and Convection. *J. Adv. Model. Earth Syst.*, *10*(3), 770–800. doi: 10.1002/2017MS001162

Thuburn, J., Weller, H., Vallis, G. K., Beare, R. J., & Whitall, M. (2018). A Framework for Convection and Boundary Layer Parameterization Derived from Conditional Filtering. *J. Atmos. Sci.*, *75*(3), 965–981. doi: 10.1175/JAS-D-17-0130.1

Troen, I. B., & Mahrt, L. (1986). A simple model of the atmospheric boundary layer; sensitivity to surface evaporation. *Bound.-Lay. Meteorol.*, *37*(1), 129–148. doi: 10.1007/BF00122760

Turner, J. S. (1979). *Buoyancy Effects in Fluids*. Cambridge University Press.

Vallis, G. K. (2017). *Atmospheric and oceanic fluid dynamics*. Cambridge University Press.

Van Roekel, L., Adcroft, A. J., Danabasoglu, G., Griffies, S. M., Kauffman, B., Large, W., ... Schmidt, M. (2018). The KPP Boundary Layer Scheme for the Ocean: Revisiting Its Formulation and Benchmarking One-Dimensional Simulations Relative to LES. *J. Adv. Model. Earth Syst.*, *10*(11), 2647–2685. doi: 10.1029/2018MS001336

Weiss, W. (1994, February). The balance of entropy on earth. *Continuum Mech. Thermodyn*, *8*(1), 37–51. Retrieved 2024-07-04, from http://link.springer.com/10.1007/BF01175750 doi: 10.1007/BF01175750

Weller, H., McIntyre, W., & Shipley, D. (2020, August). Multifluids for Representing Subgrid-Scale Convection. *Journal of Advances in Modeling Earth Systems*, *12*(8). Retrieved 2021-11-01, from https://onlinelibrary.wiley.com/doi/10.1029/2019MS001966 doi: 10.1029/2019MS001966

Witek, M. L., Teixeira, J., & Matheou, G. (2011). An Eddy Diffusivity–Mass Flux Approach to the Vertical Transport of Turbulent Kinetic Energy in Convective Boundary Layers. *J. Atmos. Sci.*, *68*(10), 2385–2394. doi: 10.1175/JAS-D-11-06.1

Wu, X., & Yanai, M. (1994). Effects of Vertical Wind Shear on the Cumulus Transport of Momentum: Observations and Parameterization. *J. Atmos. Sci.*, *51*(12), 1640–1660. doi: 10.1175/1520-0469(1994)051⟨1640:EOVWSO⟩2.0.CO;2

Yano, J.-I. (2014). Formulation structure of the mass-flux convection parameterization. *Dynam. Atmos. Oceans*, *67*, 1–28. doi: 10.1016/j.dynatmoce.2014.04.002

Zhang, M., Somerville, R. C. J., & Xie, S. (2016, April). The SCM Concept and Creation of ARM Forcing Datasets. *Meteorol. Monogr.*, *57*(1), 24.1–24.12. doi: 10.1175/AMSMONOGRAPHS-D-15-0040.1